Journal of Cancer Stem Cell Research (2014), 2:e1006
 ISSN 2329-5872
DOI: 10.14343/JCSCR.2014.2e1006
http://cancerstemcellsresearch.com

Research Article Open Access

Distinct molecular signature of recurrent ovarian tumor cells isolated from the ascites of advanced-stage serous ovarian cancer patients

Ardian Latifi[1,2], Ruth Escalona[1], Michael A Quinn[1,3], Erik W Thompson[2,4], Jock K Findlay[1,3,5] and Nuzhat Ahmed[1,2,3,5,*]

[1]Women's Cancer Research Centre, Royal Women's Hospital, Victoria 3052, Australia, [2]Department of Surgery, St Vincent Hospital, University of Melbourne, [3]Department of Obstetrics and Gynaecology, University of Melbourne, Victoria 3052, Australia, [4]St Vincent's Institute, Victoria 3065, Australia and [5]MIMR-PHI Institute of Medical Research, Victoria 3168, Australia

Abstract: Seventy percent of ovarian cancer patients die due to consecutive episodes of recurrences resulting from the re-growth of ovarian tumor cells resistant to conventional chemotherapies. In an effort to identify chemoresistance mechanisms, we compared the expression of genes in tumor cells isolated from the ascites of advanced-stage serous ovarian cancer patients prior to (chemonaive, CN) and after chemotherapy treatments (chemoresistant/recurrent, CR). A novel, recently published method was used for the isolation of tumor cells from the ascites of CN and CR patients. Illumina HT-12 platform was used to assess the differential expression of genes (DEGs) between the isolated tumor cells from the ascites of CN and CR patients. The identification of DEGs was achieved by comparing the genetic signatures of CN versus CR samples by a mean expression ratio (fold change) of 2 and $P < 0.05$. Validation of selected genes was performed by quantitative Real Time Polymerase Chain Reaction (qRT-PCR). The dominant canonical pathways in the CR versus CN tumor cells were determined by Ingenuity Pathway Analysis. Gene expression analysis revealed differential expression of 414 genes, with 179 genes up regulated and 235 down regulated in the CR group. There were significant differences in gene expressions encoding for proteins involved with cancer stem cells, cell-cell adhesion, embryonic development, tumor suppression, immune surveillance, retinoic acid and energy metabolism in tumor cells isolated from CR compared to CN patients. Pathway analysis revealed that changes in cell cycle pathways, prominently those involved with mitosis and polo-like kinase (*PLK1*), G2/M DNA damage and proteins linked with cell cycle checkpoint regulation associated with chemoresistance. This preliminary molecular profiling, on a small number of patient samples, suggests an important discrimination of genes in the isolated tumor cells derived from the ascites of CN and CR patients. This type of study on a larger cohort of samples may have important clinical implications for the development of therapeutic strategies to overcome chemoresistance and associated recurrences in ovarian cancer patients.

Keywords: ovarian cancer, cancer stem cells, metastasis, ascites, chemoresistance, recurrence.

INTRODUCTION

Ovarian cancer represents 3% of all the new cancer cases in American women, but accounts for 5% of all the cancer-related deaths [1]. This discrepancy occurs due to the resistance of ovarian cancer patients to current chemotherapy regimens resulting in the deaths of 70% of the patients within the first five years of diagnosis [2]. The vast majority of ovarian cancer patients diagnosed with an advanced-stage disease undergo debulking surgery followed by adjuvant chemotherapy consisting of a platinum agent (typically carboplatin) alone or in combination with a taxane (paclitaxel) [2]. Initially, seventy percent of the women respond to this therapy, but unfortunately the majority of these patients eventually relapse due to drug-resistant recurrent disease and die due to peritoneal metastasis [3]. Disappointingly, the five year survival period of these patients has remained unchanged and as low as ~30% for the last thirty years [4].

Metastasis in ovarian cancer is unique as it is usually localized within the peritoneal cavity and derives directly from the ovaries and/or the fallopian tubes to the adjacent organs (extraovarian pelvic organs, colon, bladder and liver) and/or by the attachment of exfoliated cancer cells which survive as cellular aggregates and are carried by the peritoneal tumor fluid (ascites) to surrounding organs in the peritoneal cavity [5–8]. The presence of ascites is associated with a poor prognosis [4, 9]. Microscopic

*Corresponding author: Dr Nuzhat Ahmed, Women's Cancer Research Centre, Royal Women's Hospital, 20 Flemington Road, Parkville, Vic 3052, Australia. Telephone: 61 3 8345 3734; E-mail: nuzhat.ahmed@thewomens.org.au
Received: July 9, 2014;
Accepted: October 5, 2014

inspection of ascites display a complex heterogeneous picture of cellular environment constituting single cells, floating multicellular aggregates of non-adherent cells, cancer-associated fibroblasts, myeloid cells, activated mesothelial cells and cancer stem cells (CSCs) [10–12]. Extensive seeding of these floating cells on the uterus, sigmoid colon and omentum is frequently encountered in advanced-stage and recurrent patients and ultimately leads to disruption of major organs and eventually death [7]. During the course of recurrence, cells within the small microscopic residual cellular aggregates release soluble pro-angiogenic mediators, which diffuse out from the tumor population and bind to endothelial cells of mature blood vessels leading to angiogenesis, which sets the tumor expansion and recurrence in motion [13]. Hence, the presence of floating cellular aggregates, commonly known as spheroids, in the ascites of ovarian cancer patients is strongly associated with recurrence, and there is an urgent need to study these spheroids in the ascites in order to establish the mechanisms of recurrence.

Mechanisms underlying the development of resistance to platinum-based agents have been well characterized in other cancers and include DNA repair mechanisms, altered cellular transport of the drugs, increased antioxidant production, and reduction of apoptosis [14–16]. Elevated gene expression affecting cellular transport, DNA repair, apoptosis, cell-extracellular matrix and cell-cell adhesion has been observed in ovarian cancer patient's samples resistant to platinum-based therapy [17–19]. Taxanes were originally used as an alternative to platinum based agents in order to overcome platinum resistance in patients [20]. The development of taxane resistance has also been well studied and characterized [21, 22]. Typical mechanisms of paclitaxel resistance involve alteration in drug transport, altered expression of microtubule proteins, expression of taxane metabolizing proteins and altered cell signaling resulting in reduced apoptosis [22–25]. The roles of some of these factors in cancer patients in response to taxane treatment (e.g. altered expression of class III β-tubulin, reduced apoptosis conferred by survivin expression and metabolism of taxanes by cytochrome P450 reductase) have also been implicated in clinical samples [23–25].

It is still not known if the mechanisms of resistance to 'combination chemotherapy' are a combined response of tumor cells to single agents or if a novel mechanism of resistance exists that is different from the resistance mechanisms observed with single agents. In recent studies, we have demonstrated ovarian CSCs to be involved with resistance to both platinum and taxane-based chemotherapies [26, 27]. We and others have also shown recurrent ovarian tumors to be enriched with CSCs and mediators of pathways that regulate CSCs, suggesting that CSCs may contribute to the development of recurrence [10, 11, 28, 29].

To date most of the research conducted to understand the chemoresistance mechanisms have used cancer cell lines and few data are available on the relevance of these studies on the potential mechanisms of chemoresistance in clinical samples [30, 31]. In recent studies, gene expression profiles of chemonaive (primary tumors obtained during debulking surgery) and post chemotherapy tumors have been analyzed to determine the molecular signature/s associated with chemoresistance [17, 32]. These studies, although important, used tumor sections, which are likely to present a complex molecular profile of not only chemoresistant tumor cells but also associated stroma and infiltrated cells. As a consequence, these mixed genetic profiles may not truly represent the associated pathways regulating chemoresistance in tumor cells; hence, such results may misrepresent the targets proposed for future therapeutic interventions. Isolated tumor cells that survive chemotherapy treatments in patients are likely to experience changes in gene expression allowing them to withstand the selective pressure of the drugs. These phenotypically changed tumor cells are likely to exhibit a molecular signature associated with chemoresistance when compared to the gene expression profile of isolated tumor cells before chemotherapy treatment.

In the present study, we have used our recently described novel separation technique to isolate tumor cells from the ascites of advanced-stage CN and CR serous ovarian cancer patients [10]. Ascites samples were collected from patients (not matched) at the time of surgery prior to chemotherapy treatment (CN) and at different time points during recurrence (CR). In this preliminary study, changes in gene expression associated with chemoresistance and recurrence were analyzed on a small set of unmatched CN ($n = 4$) and CR ($n = 4$) samples by a microarray gene expression profiling method. This study aimed to (i) identify the molecular signature associated with the isolated ascites-derived tumor cells of CR patients; (ii) provide novel information about specific genes that regulate the chemoresistant/recurrent phenotype of ascites-derived CR tumor cells, and (iii) provide an insight into cellular pathways that regulate chemoresistance in ascites-derived CR ovarian tumor cells. Our data identified novel genes and associated pathways which may have clinical relevance in designing therapeutic interventions for ovarian cancer patients. To our knowledge this is the first study, which has demonstrated a distinct molecular profile of isolated tumor cells from the ascites of CR patients.

MATERIALS AND METHODS

Patient Recruitment

Ascites were collected from patients diagnosed with advanced-stage serous ovarian adenocarcinoma after obtaining written informed consent under protocols approved by the Research and Human Ethics Committee

Table 1. Description of serous ovarian cancer patients recruited for this study

Samples	Stage	Grade	Age	Time of first recurrence (after completion of first line of chemotherapy)	Time of sample collection (after diagnosis)	Patient status	Treatment received before the collection of ascites	Study technique used
As31	IIIc	*G3	54	NA	AD	CN	None	Microarray
As36	IIIc	*G3	59	NA	AD	CN	None	Microarray and validation
As37	IIIc	*G3	48	NA	AD	CN	None	Microarray and validation
As35	IIIc	*G3	90	NA	AD	CN	None	Microarray and validation
As59	IIc	*G3	64	NA	AD	CN	None	Validation
As82	IIIc	*G3	48	NA	AD	CN	None	Validation
As86	IIIa	Unknown	51	NA		CN	none	Validation
As22C	IIIc	Unknown	54	1 month	10 months	#CR	Carboplatin and Paclitaxel (3 cycles), Doxorubicin (4 cycles), AMG386 Topotecan (2 cycles), Cyclophosphamide (2 cycles)	Microarray and validation
As22D	IIIc	Unknown	54	1 month	11 months	#CR	Carboplatin and Paclitaxel (3 cycles), Doxorubicin (4 cycles), AMG386 Topotecan (2 cycles), Cyclophosphamide (3 cycles)	Microarray
As34	Unknown	*G3	65	4 months	1 year	#CR	Carboplatin and Paclitaxel (6 cycles)	Microarray and validation
As39	Unknown		80	7 months	1 year 5 months	#CR	Carboplatin and Paclitaxel (6 cycles), Liposomal Doxorubicin (6 cycles)	Microarray and validation
As60	IIIc	*G3	52	4 months	2 years	#CR	Cisplatin and Paclitaxel (6 cycles), AMG-386 182 (Clinical Trial, 8 cycles)), Paclitaxel (3 cycles), Paragon Trial (Anastrozole, 2 Cycles), Cisplatin (3 cycles)	Validation
As72	IIIc	*G3	62	8 months	2 years 9 months	#CR	Carboplatin and Paclitaxel (6 cycles), Gemcitabine and Carboplatin (6 cycles)	Validation
As73	IIIc	*G3	56	6 months	2 years 9 months	#CR	Carboplatin and Paclitaxel (6 cycles), AMG-386 182 Trial (9 cycles), Paclitaxel (6 cycles), Cyclophosphamide (2 cycles), Topotecan (2 cycles), Liposomal Doxorubicin (2 cycles)	Validation

*G3-Poorly differentiated; NA-Not applicable; #CR - ascites was collected after the patients had undergone the above described cycles of chemotherapy; AD-After diagnosis, before treatment.

(HEC # 09/09) of The Royal Women's Hospital, Melbourne, Australia. The histopathological diagnosis, tumor grades and stages were determined by independent staff pathologists as part of the clinical diagnosis. Ascites (As) samples (500 ml-2L) were obtained during surgery from patients with primary carcinoma (n = 7), and at the time of recurrence (n = 6) (Table 1). Apart from As22 which was collected twice from the same patient (As22C and D) during sequential ascites removal within a month, other samples were from individual cases. CN patients (n = 7) did not receive any chemotherapy. All CR patients (n = 6) were diagnosed with a recurrent disease within 1–8 months after completion of their first line of chemotherapy treatment (Table 1). These patients had partial response to the first and subsequent lines of chemotherapy. The chemotherapy agents administered to patients, and the number of chemotherapy cycles varied from patient to patient and are indicated in Table 1. In CR group, ascites was collected from patients at recurrence after the patients have received the cycles of chemotherapy described in Table 1.

Isolation of tumor cells from the ascites of ovarian cancer patients

Tumor cells from ascites were separated using the method described previously [10]. Briefly, cells were collected from ascites by centrifugation and cleared of red blood cells by hypotonic shock. The remaining cells were then cultured on 6-well low attachment plates for 3–4 days and both adherent (non-tumorigenic, stromal cells) and non-adherent (tumorigenic) cells were screened for fibroblast

surface protein (FSP), cancer antigen 125 (CA125) and cytokeratin 7 (CK7) by flow cytometry to assess the purity of each fraction [10]. The non-adherent epithelial tumorigenic population rich in CK7 and CA125 and lacking FSP and vimentin was processed further for microarray analysis.

Flow cytometry analysis

The flow cytometry method has been described previously [33]. All data were analysed using Cell Quest software (Becton-Dickinson, Bedford, MA, USA). Results are expressed as mean intensity of fluorescence (MIF).

Immunofluorescence analysis

Immunofluorescence analysis was performed as described previously [33]. Images were captured using the Leica TCS SP2 laser, and viewed on a HP workstation using the Leica microsystems TCS SP2 software.

RNA extraction and microarray analysis

Isolated tumor cells were homogenised in TRIzol. RNA extracts >3 μg from clinical samples (Table 1) were outsourced to Australian Genome Research Facility (AGRF) Melbourne, Australia for microarray processing. The Illumina (Sentrix Human HT12v4) platform with 47,232 probes was used as described before [34, 35]. Briefly, the Agilent BioAnalyser 2100 was used to determine the quality and integrity of the RNA using the NanoChip method (Agilent Technologies, USA). A total of 500 ng of RNA was labeled using the Total Prep RNA amplification kit (Ambion, USA). 1.5 ug of labeled cRNA was prepared for hybridisation to the Sentrix Human-HT12 Beadchip by preparing a probe cocktail that included GEX-HYB Hybridisation Buffer (Illumina).

A total hybridisation volume of 30 μl was loaded into a single array on the Sentrix Human-HT12 Beadchip. The chip was hybridised at 58ºC for 16 h in an oven with a rocking platform and washed using the appropriate protocols as outlined in the Illumina manual (http://support.illumina.com/documents/MyIllumina/3466bf71-78bd-4842-8bfc-393a45d11874/WGGEX_Direct_Hybridization_Assay_Guide_11322355_A.pdf), and then coupled with Cy3 and scanned in the Illumina iScan scanner. The scanner operating software, GenomeStudio was used to process measured signal intensities into a text file for analysis.

Analysis of the microarray data

This was performed by AGRF. Raw signal intensity data from Illumina HT-12 slides (www.illumina.com) were background corrected within GenomeStudio. Mean signal intensities were calculated per sample. Individual signal intensities were floored to a value 10% of the mean signal intensity of the array, i.e. to a value of 40. This step was performed to eliminate negative expression values where original, non-background subtracted intensities were within the background range. Data were log2 transformed, and quantile normalized in Partek Genomics Suite 6.5 (www.Partek.com). Only probes with a coefficient of variation of more than 5% were further considered (n = 17,163). A t-test assuming unequal variance was performed, with a bootstrap multiple testing correction (200 randomizations). Gene ontology enrichment analysis was performed in Partek (Genomics Suite 6.5), using either the default gene ontology categories or the KEGG GO database (www.genome.jp/kegg/). Enrichment Fisher exact p-value was calculated based on the number of genes in the provided gene list in relation to the number of genes in gene groups in the genome annotation file. The enrichment score was calculated as negative antilog of that p-value. The larger the enrichment score, the higher the enrichment of that functional group in the provided gene list.

The identification of DEGs was achieved by comparing the genetic signatures of CN versus CR samples and was defined by a mean expression ratio (fold change or FC) of 2 and a P-value cut-off of 0.05. The gene expression data was analyzed using the established two-dimensional hierarchical clusters of genes in the form of a color-coded Heat Map. A Principal Component Analysis (PCA) generated by Partek Genomics Suite 6.6 was used to translate the data into a three-dimensional image whereby the dimensionality of the data set was reduced to a sphere-like representation while maximizing the discrimination between the groups [36].

Ingenuity pathway analysis

The molecular interactions of the canonical pathways between the tumor cells of CN and CR ovarian cancer patients was established by correlating the results obtained from the gene expression data with genes whose biological functions are known in the literature using Ingenuity Pathway Analysis (http://www.ingenuity.com). The CR-associated DEGs list containing the 414 unique genes was filtered using the criteria of FC > 2 and P < 0.05. Ingenuity recognizes the Illumina identifiers and generated common pathways or molecular connections between the CR and CN isolated ascites tumor cells. Representations of the molecular relationship between CN and CR ascites tumor cells were generated based on FC > 2 and P < 0.05 using Benjamini-Hochberg multiple resting correction values.

Quantitative Real Time Polymerase Chain Reaction (qRT-PCR) Analysis

Validation of selected genes identified by microarray analysis was performed by qRT-PCR. RNA was extracted from ascites-derived tumor cells using TriZol from the six different CN and CR patients described in Table 1. Extracted RNA was quantified using the NanoDrop-2000 Spectrophotometer (NanoDrop Technologies INC). RNA quality and integrity were verified by agarose gel electrophoresis. Complementary DNA (cDNA) was

Table 2. Human oligonucleotide primer sequences for quantitative real-time PCR

Gene Symbol	Accession no.	Primer sequences from 5′-3′	Size (bp)	Data Capture Temp (°C)
ADAMTS9	NM_182920.1	Forward CGAAAAACCTGCCGTAATGT Reverse TCAGAGTCTCCATGCACCAG	191	78
BCL11A	NM_022893.3 NM_018014.3 NM_138559.1	Forward CTCTCCTCCCCTCGTTCTG Reverse CTTCCGTGTTCGCTTTCTAAGTA	206	80
CLDN1	NM_021101.4	Forward ACTCCTTGCTGAATCTGAGCAGC Reverse CCAGTGAAGAGAGCCTGACC	301	81
CLDN16	NM_006580	Forward CTCCCTGATGAGCCGTACAT Reverse AGAACAGCTCCAGCCAAAAA	233	80
CRABP2	NM_001878.3 NM_001199723.1	Forward CGGAAAACTTCGAGGAATTG Reverse CATCCACAGTCTGCTCCTCA	198	80
PAX8	NM_003466.3	Forward AAGGTGGTGGAGAAGATTGG Reverse GCTGCTCTGTGAGTCAATGC	387	82
PROM1	NM_006017	Forward ATTGGCATCTTCTATGGTTT Reverse GCCTTGTCCTTGGTAGTGT	167	78
Rn18S	NR_003286.1	Forward GTAACCCGTTGAACCCCATT Reverse CCATCCAATCGGTAGTAGCG	153	80
SerpinA3	NM_001085.4	Forward GCTCATCAACGACTACGTGAA Reverse CACCATTACCCACTTTTTCTTGC	190	78
TGFBR3	NM_003243.2	Forward ACATGGATAAGAAGCGATTCAGC Reverse AACGCAATGCCCATCACGGTTA	331	80

synthesized from 500 ng of RNA using the High Capacity cDNA Transcription Kit (Applied Biosystmes, CA, USA) as per manufacturer's instructions. PCR reactions were performed in triplicate with negative controls where water was used in place of reverse-transcribed template included for each primer pair to exclude PCR amplification of contaminating DNA. The primers used for qRT-PCR are summarized in Table 2. A PCR product was amplified for each set of primers, purified using the QIAquick® Gel Extraction Kit (Qiagen), quantified using the NanoDrop-2000 Spectrophometer and verified by size by agarose gel electrophoresis. The PCR product was then diluted from 500 fg to 0.5 fg and was used as a standard for quantitative analysis. Absolute quantification of PCR products was performed as described previously [37].

RESULTS

Morphology of cells collected from the ascites of ovarian cancer patients

Ascites cells derived from both CN (n = 4) and CR patients (n = 3) were assessed by phase contrast microscopy after seeding on low attachment plates for 24 h. Two distinct populations of cells were observed: (i) multicellular aggregates (spheroids) that floated as three-dimensional structures in the growth medium without attachment (Figure 1A), and (ii) spindle shaped fibroblast-like single cells that adhered to the low attachment plates (Figure 1C).

Morphological assessment of the spheroids revealed a three dimensional cluster of cells loosely compacted together and surrounded by layers of cells (Figure 1A). In general spheroids were in the form of loose aggregates

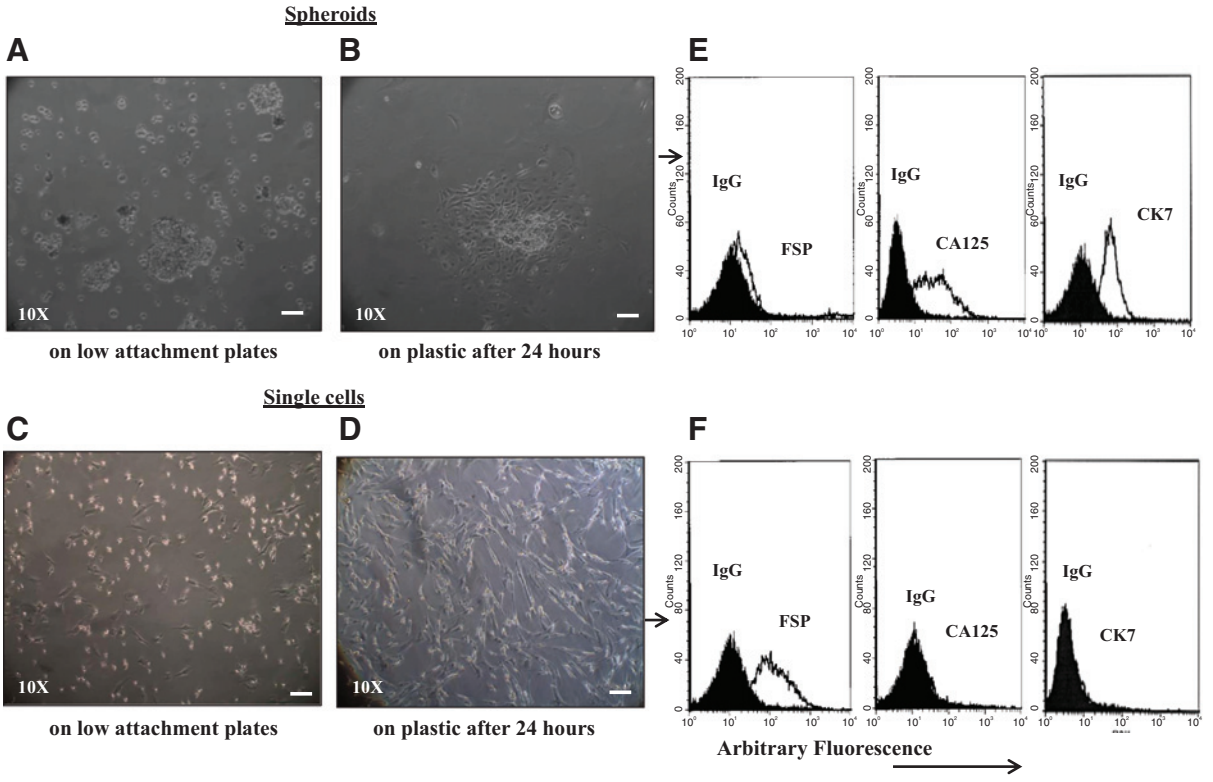

Figure 1. Morphological features and expression of surface markers of ascites-derived spheroids and single cells. (**A**) Spheroids and (**C**) single cells were seeded on low attachment plates immediately after collection. Morphological features of (**B**) spheroids and (**D**) single cells on tissue culture plastic after 24 h following seeding. Images were assessed by a phase contrast microscope. Magnification was 100x, scale bar = 50 µm. The images are representative of n = 14 samples. (**E-F**) Flow cytometric assessment of purified cells from the ascites of CN (n = 7) and CR (n = 7) ovarian cancer patients was performed by incubating the cells with either control IgG or relevant primary antibodies against the respective antigens followed by incubation with secondary phycoerythrin conjugated antibody. Results are representative of (n = 14) independent samples. The filled histogram in each figure represents control IgG, black lines indicate protein expression in respective cells.

of small clusters of cells with a defined outer rim (Figure 1A). After 24 h on tissue culture plastic, most spheroids attached to the plates and there was a transformation from a three dimensional structure to flattened cellular clusters containing several layers of cells adherent on top of each other (Figure 1B). The periphery of the spheroids showed thin elongated cells moving out of the spheroid whereas cells towards the centre were more rounded in structure. As the cells moved away from the centre, cell-cell contact was reduced resulting in the slow disaggregation of the spheroid (Figure 1B). On the other hand, single cells attached to the plastic as elongated spindle-like cells having a fibroblast-like morphology (Figure 1D).

Assessment of cell surface markers by flow cytometry

Single cells and spheroids (dispersed by trypsinization) were characterized by the cell surface expression of FSP, CA125, and CK7 by flow cytometry. High expression of CA125 and CK7 was observed in the cells dispersed from spheroids, while no expression of FSP was evident (Figure 1E). On the other hand, the single cells were positive for FSP and no expression of CA125 and CK7 was evident (Figure 1F).

Analysis by immunofluorescence

We next analyzed the expression and localization of vimentin in ascites samples by immunofluorescence. Consistent with the flow cytometry results, no expression of vimentin was observed in the cells within the spheroids (Figures 2B-C). Vimentin expression was only evident in cells protruding out of spheroids (Figures 2B-C). On the other hand, single cells demonstrated strong expression of vimentin (Figure 2E-F). Vimentin expression was evident in both cytoplasm and membrane of single cells (Figures 2E-F).

Heat Map and Principal Component analysis

Eight ascites-derived spheroid tumor samples were used to determine the gene expression changes in CN and CR tumor cells derived from the ascites of ovarian cancer patients. A pool of 47,232 probes was used to assess the expression of 18,009 genes. To analyse the variation in gene expression between the CN and CR groups, two dimensional colour-coded Heat Maps were generated using the filtering criteria of FC $>$ 2 and P $<$ 0.05 (Figure 3). The genes represented in yellow are up regulated, while those represented in red are down regulated in the respective CN or CR groups. The Heat Map demonstrated a distinct separation of genes in CN

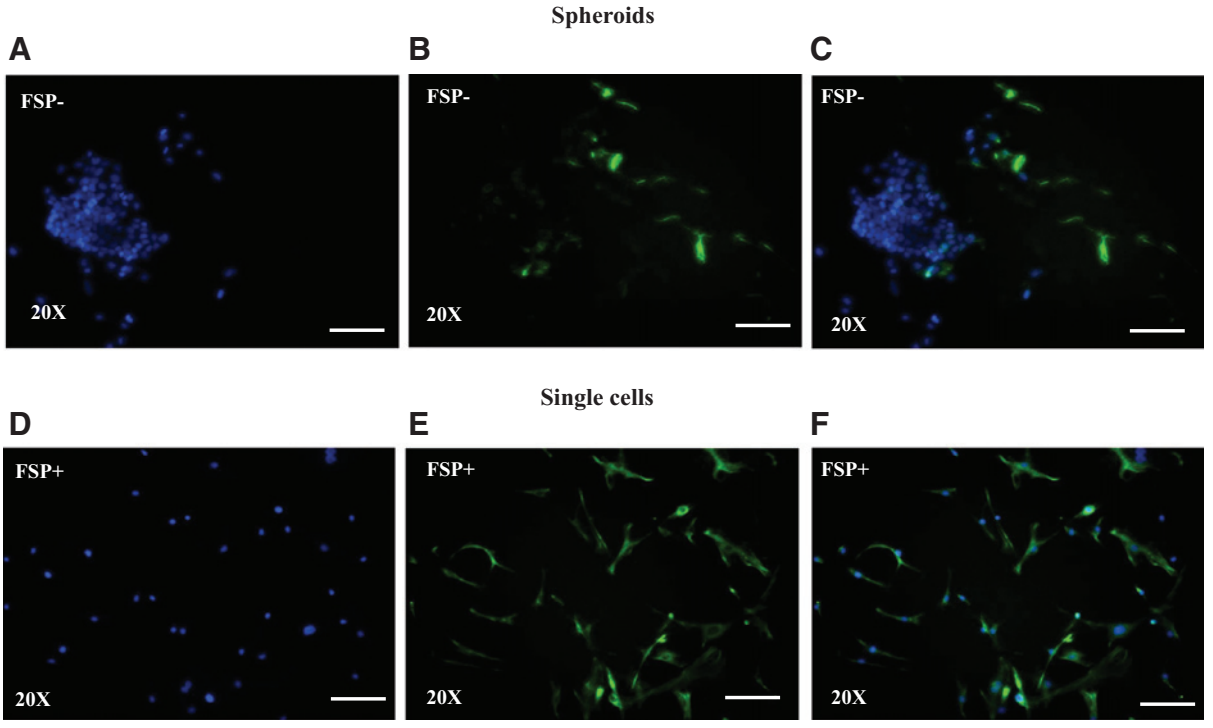

Figure 2. Expression of vimentin in spheroids and single cells. (A-F) Purified spheroids and single cells were evaluated for the expression and localization of vimentin by immunofluorescence using mouse monoclonal antibody (green) as described in the Methods and Materials. Cellular staining was visualized using the secondary Alexa 488 (green) fluorescent labeled antibody, and nuclear staining was detected by DAPI (blue). **A** and **D**, cells were only stained with DAPI (blue), **B** and **E**, cells were stained with anti-vimentin followed by Alexa 488 (green), **C** and **F** overlay of DAPI and vimentin staining. Magnification was 200x; scale bar = 50 μm.

and CR tumor groups. Genes which were up regulated in the CR group were down regulated in the CN group and vice versa, suggesting that these two groups are distinctly different from each other (Figure 3A). This was supported by the PCA mapping of 83.4% obtained between the CN and CR spheroid tumor samples (Figure 3B). These observations were consistent with PC1 values of 70.1% along the x-axis which indicates significant genetic variation between the CN and CR groups, while the small PC2 variation of 6.66% indicates small variation of samples within the same groups.

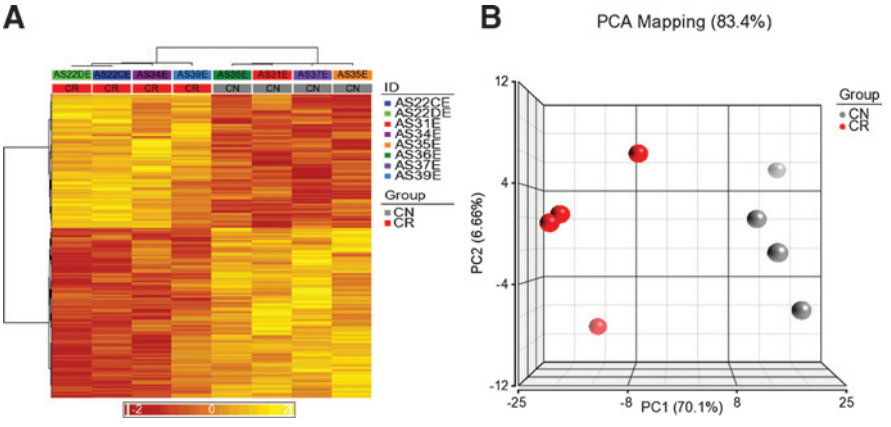

Figure 3. Differential expression of genes (DEGs) in CN and CR samples. (A) The Heat Map analysis of genes was performed at $P < 0.05$ and Fold Change >2. The gene expression analysis is based on 433 probes representing 414 DEGs. DEGs in the CN and CR samples are displayed in a color-coded matrix which is divided into four large rectangular boxes representing the up regulated (yellow) or down regulated (red) genes. The columns along the x-axis (from right to left), are the clinical samples [CN n = 4, followed by CR (n = 4)]. The intensity of colors are indicative of how positively (yellow) or negatively (red) these 414 genes are detected by 433 probes. **(B):** PCA analysis of genes at $P < 0.05$ and fold change >2. The PCA which contributes to the overall differences in the CN and CR groups is noted at the top of the graph. Variation between the CN (grey) and CR (red) groups are indicated by spheres.

Table 3. 20 most up regulated genes in CR compared to CN ascites tumor cells (FC > 2, P < 0.05)

Gene Symbol	Probe ID	P-value	FC	Gene Name	Gene Function
CLDN16	5960102	0.013	26.39	Claudin16	Cell-cell adhesion [38]
ADAMTS9	1570382	0.002	22.40	A disintegrin and metalloproteinase with thrombo-spondin type 1, motif 9	Involved in the cleavage of proteoglycans, the control of organ shape during development, and inhibition of angiogenesis [43, 79]
UCA1	4250367	0.015	18.88	A non-protein-coding RNA	Embryonic development and cancer associated RNA [42]
CLDN1	5960296	0.030	16.49	Claudin1	Cell-cell adhesion [39]
LAMA3	6480592	0.026	16.00	Laminin,alpha3	Mediate attachment, migration, organization of cells during embryonic development [40]
LAMA3	2650612	0.040	12.11	Laminin,alpha3	Same as above
LOC651957	5560707	0.008	11.70	Unknown	Unknown
C140RF78	3390551	0.041	10.84	AHNAK nucleoprotein	Calcium channel regulators [46]
CPNE8	1470386	0.042	10.34	Copine 8	Phospholipids binding protein [45]
AHNAK2	5260594	0.023	10.08	AHNAK nucleoprotein	Calcium channel regulators [46]
KIF13B	5290209	0.008	9.78	Kinesin family member 13B	Transport of phosphatidylinosito (3,4,5)-triphosphate in neurons
PAX8	4850070	0.030	9.53	Paired box 8	Embryonic developmental gene frequently expressed in cancer including ovarian cancer [44, 87]
PROM1	7400452	0.022	9.33	Prominin1, CD133	Transmembrane protein expressed on adult stem cells. Suppresses differentiation [100, 101]
CPNE8	580592	0.045	9.13	Copine 8	Phospholipids binding protein [45]
TGFβR3	3190379	0.036	6.70	Type III transforming growth factor-beta receptor (betaglycan)	Embryonic development and loss of the receptor in cancer [43, 92]
C200RF46	730491	0.016	5.32	Unknown	Unknown
LIPG	7210681	0.046	5.94	Endothelial lipase	Intravascular modelling of lipoproteins [47]
C1ORF116	730491	0.016	5.32	Unknown	Unknown
LOC642299	6020561	0.024	5.15	Unknown	Unknown
SLC16A5	6860082	0.0192	5.14	Solute carrier family 16 (monocarboxylate transporter) member 5	Involved in the transport of monocarboxylate across the plasma membrane. It is postulated that it has function in the disposition of drugs [48]

Changes in gene expression associated with chemoresistance and recurrence in isolated ascites tumor cells

A total of 414 genes were identified to be differentially expressed between the CN and CR groups. Of these 190 probes representing 179 genes were up regulated and 243 probes representing 235 genes were down regulated in the CR spheroid tumor samples. The 20 most up regulated or down regulated genes are presented in Tables 3 and 4, respectively. Of the 20 up regulated genes, 4 genes were unknown (Table 3). Three genes, *LAMA3*, *CPN8* and *PAX8*, were identified twice with different probes. Genes involved with cell-cell adhesion such as *CLDN16*, *CLDN1*, *LAMA3* [38–40] and inhibition of metastasis and angiogenesis, *ADAMTS9* [41] topped the list (Table 3). This was followed by genes involved in embryonic development such as *UCA1* [42], *TGFβR3* [43] and PAX8 [44]. In addition, phospholipid binding protein *CPNE8* [45], calcium channel regulators *AHNAK2* [46], proteins involved with intravascular modelling of lipoproteins, *LIPG* [47] and monocarboxylate transporter, SLC16A5 [48] were also included in the list (Table 3).

Of the twenty most down regulated proteins, *Serpin A3* involved with inflammatory reactions topped the list [49] (Table 4). The majority of the proteins in the twenty most down regulated list were associated with tumor infiltration and endothelial cells as well as host immunity. These included *HCLS1* [50], *SOX 18* [51], *HOXB5* [52], *HLA-DRB4* [53], *LY9* [54], *IF116* [55], *CD99* [56], and *BCL11A* [57]. Tumor suppressor genes such as *FBP1* [58], *RASSF2* [59] were also included in the top twenty list of down regulated genes. In addition, the cell cycle regulator *CDKN3* [60], inhibitor of cellular migration *FGD3* [61], and regulator of cytokinesis *KIF20A* [62] were also in the top 20 down regulated genes. However, *HOXB2,* which has previously been shown as a regulator in breast tumorigenesis was lost in CR ascites tumor cells [63]. In addition *GLIPR2*, a regulator of fibrosis and EMT [64], *RGS2*, a regulator of G protein signalling 2 involved with cellular stress [65] *PSRC1*, proline/serine- rich coiled-coil 1 which functions as a microtubule destabilizing protein and controls mitotic progression [66] and *PMP22*, peripheral myelin protein 22 shown to be involved with modulation of alpha6 integrin in human endometrium [67] was down regulated in CR tumors. The differential distribution of genes in the isolated CR compared to CN tumor cells obtained from the ascites of ovarian cancer patients is demonstrated in Figure 4. The microarray expression data has been uploaded as Supplementary Table 1.

Table 4. 20 most down regulated genes in CR compared to CN ascites tumor cells (FC > 2, P < 0.05)

Gene Symbol	Probe ID	P-value	FC	Gene Name	Gene Function
SerpinA3	6280168	0.0056	−26.39	Serine protease inhibitor3	Associated with the inflammatory reactions [49]
HOXB2	3460097	0.030	−16.46	Homeobox transcription factor 2	Involved in normal development and cancer [63]
HCLS1	1300408	0.018	−9.00	Hematopoietic cell-specific Lyn substrate 1	Highly expressed in human myeloid cells and involved with the endocytic pathway required for the Ag presentation of dendritic cells [50]
SOX18	6100433	0.010	−8.35	Sex determining region Y box 18	Involved with the development of lymphangiogenesis and metastasis [51]
HOXB5	1470500	0.022	−8.34	Homeobox transcription factor B5	Involved in the differentiation of angioblasts to mature endothelial cells [52]
CRABP2	3400296	0.024	−7.34	Cellular Retinoic acid binding protein 2	Involved in vitamin A homeostasis [109–110]
HLA-DRB4	7330398	0.0100	−7.33	Major histocompatibility complex, class II, DR beta 4	Involved with the presentation of class II molecules by antigen presenting cells [53]
GLIPR2	830278	0.026	−7.02	Glioma pathogenesis-related protein 2	Mediator of fibrosis and EMT [64]
PMP22	7560138	0.035	−6.60	Peripheral myelin protein 22	Expressed in myelinating neurons and pancreatic cancer [67]
RGS2	3400019	0.043	−6.50	Regulator of G protein signalling 2	Component of cellular stress [65]
LY96	70167	0.022	−6.32	Lymphocyte antigen 96	Associates with toll-like receptor 4 and confers responsiveness to lipopolysaccyaride (LPS) [54, 107]
CD99	4290097	0.011	−6.01	Cell surface glycoprotein	Involved in leukocyte migration and T cell adhesion. Also act as an oncosuppressor in osteosarcomas [56]
PSRC1	1070762	0.015	−5.75	Proline/serine- rich coiled-coil 1	Functions as a microtubule destabilizing protein that controls mitotic progression also known as DDA3 [65]
CDKN3	5260014	0.10	−5.62	Cyclin-dependent kinase inhibitor 3	Dual specificity protein phosphatase which inactivates CDK2 [60]
RASSF2	5390095	0.040	−5.52	Ras association domain family 2	Tumor suppressor gene frequently silenced in cancer [59]
BCL11A	6580450	0.0256	−5.42	B-cell CLL/lymphoma 11A (zinc finger protein)	Involved in lymphoma pathogenesis [57]
FGD3	5270619	0.006	−5.35	FYVE, RhoGEF and PH domain containing 3	Inhibit cell migration [61]
FBP1	6020224	0.042	−5.34	Fructose 1,6 phosphatase	Key energy metabolism enzyme [58]
KIF20A	1050195	0.012	−5.31	Kinesin family member 20A	Required for the mitotic exit of cells during cytokinesis [62]
IFI16	3870594	0.046	−5.26	Interferon gamma inducible protein 16	Mediates anti-inflammatory actions of type 1 interferon through suppression of activation of caspases by inflammasomes [55]

Gene ontology enrichment analysis identified three major functional types of DEGs in the CR group. These functions included cellular components (e.g. chromosomal regulation, mitosis, cytoskeletal organization, etc), biological processes (e.g. regulation of nuclear division, organelle localization, mitoses, cytokinesis, cell cycle, cellular component assembly, etc) and molecular functions (e.g. microtubule motor activity, gene transcriptional repressor activity, etc). This data has been provided in Supplementary Table 1.

Validation of candidate genes by qRT-PCR

We next selected 6 genes from the most up regulated and 3 genes from the down regulated candidates to validate using qRT-PCR. Most of the selected genes had previously been associated with ovarian cancer progression, except *ADAMTS9* which had not been linked to ovarian cancer. Twelve samples (CN = 6 and CR = 6) (Table 1) were used to validate the microarray gene expression changes in CN and CR tumor cells isolated from the ascites of ovarian cancer patients (Figure 5).

There was a significant difference in 5 out of the 6 candidate up regulated genes selected from the microarray. These genes were involved with cell-cell adhesion such as *CLDN16* ($P < 0.05$), *CLDN1* ($P < 0.01$), the tumor suppressor gene *ADAMTS9* ($P < 0.05$) involved with inhibition of metastasis and angiogenesis and genes involved in embryonic development such as *TGFβR3*

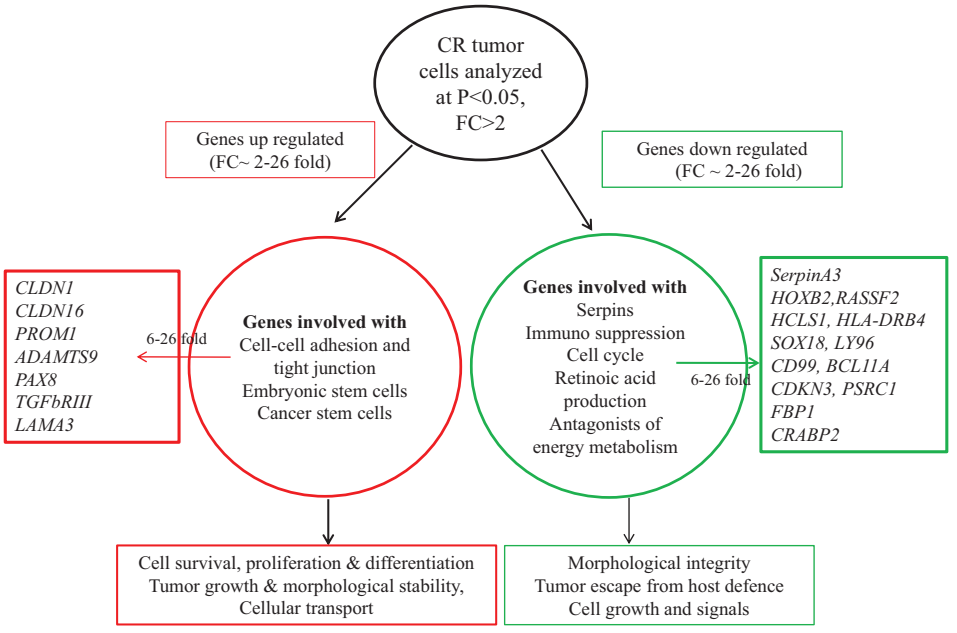

Figure 4. Differential distribution of genes in the isolated CR compared to CN tumor cells obtained from the ascites of ovarian cancer patients. Cellular functions are assigned to genes which were evaluated at $P < 0.05$ and Fold Change (FC) >2.

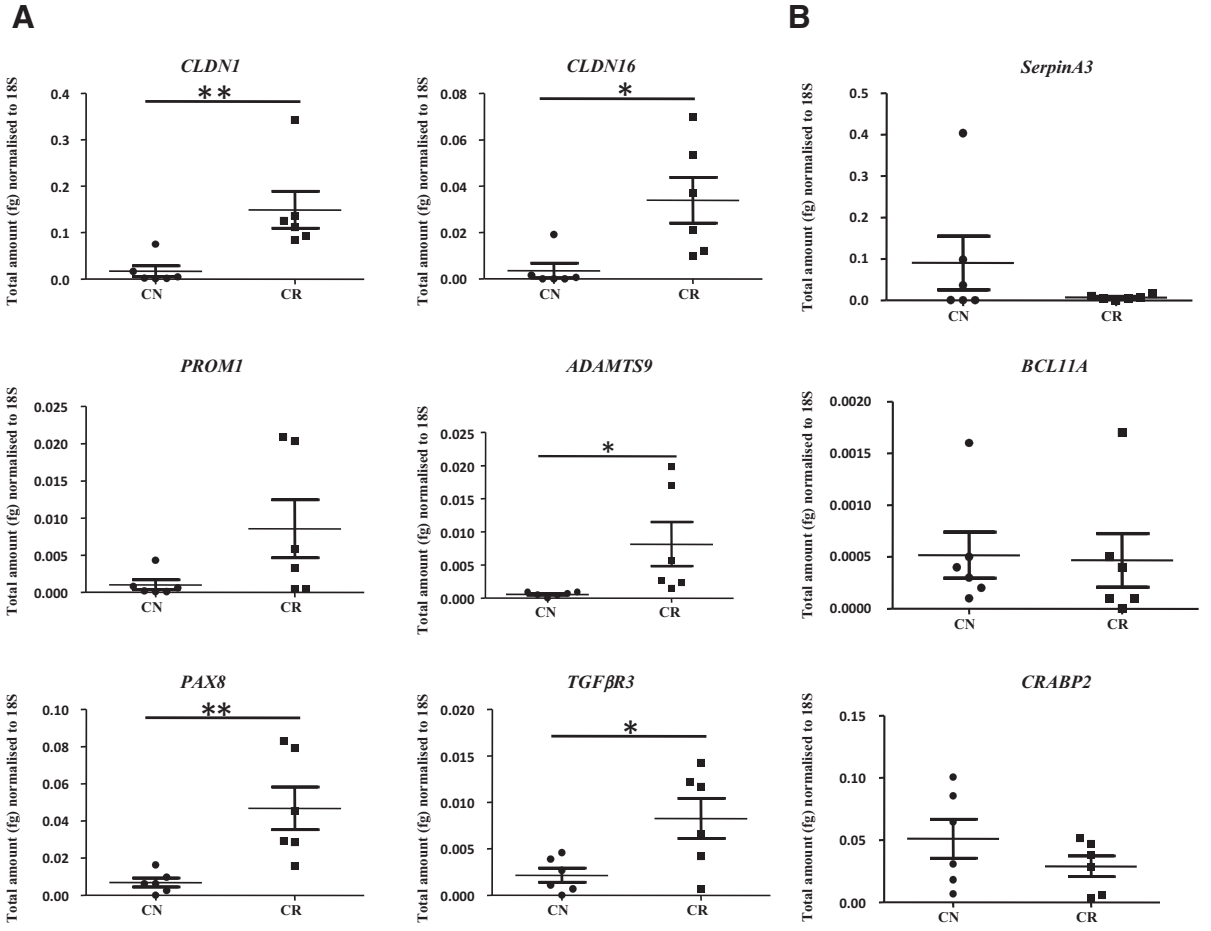

Figure 5. Validation of genes by q-PCR. (A) The absolute gene expression value of six genes up regulated and **(B)** three down regulated in CR compared to CN samples. RNA from CN (n = 6) and CR (n = 6) was extracted, cDNA was prepared and q-PCR for *CLDN-1, CLDN-16, ADAMTS9, PROM1, PAX8, TGFBR3, Serpin A3, BCL11A* and *CRABP2* was performed and the resultant mRNA levels were quantified from the standards prepared as described in the Material and Methods section. The experiments were performed on six independent CN and CR samples in triplicate. Significant intergroup variations are indicated by * $P < 0.05$, $^{**}P < 0.01$.

Table 5. 8 up regulated genes in Ass22C compared to AS22D tumor cells (FC > 2)

Gene Symbol	Probe ID	FC	Gene Name	Gene Function
APOF	130400	5.3	Apolipoprotein F	Secreted sialoglycoprotein that resides on the HDL and LDL fractions of human plasma. Human ApoF is also known as Lipid Transfer Inhibitor protein (LTIP) based on its ability to inhibit cholesteryl ester transfer protein (CETP)-mediated transfer events between lipoproteins [111]
KCNH6	7000064	3.2	Potassium voltage-gated channel, subfamily H, member 6	Voltage-gated potassium channels functions include regulating neurotransmitter release, heart rate, insulin secretion, neuronal excitability, epithelial electrolyte transport, smooth muscle contraction, and cell volume [112].
KYNU	3460685	3.4	Kynureninase	Is a pyridoxal-5′-phosphate (pyridoxal-P) dependent enzyme that catalyzes the cleavage of L-kynurenine and L-3-hydroxykynurenine into anthranilic and 3-hydroxyanthranilic acids, respectively. Kynureninase is involved in the biosynthesis of NAD cofactors from tryptophan through the kynurenine pathway [113]
LRAP	1010296	3.5	ERAP2 endoplasmic reticulum aminopeptidase 2	Aminopeptidases hydrolyze N-terminal amino acids of proteins or peptide substrates. Major histocompatibility complex (MHC) class I molecules rely on aminopeptidases such as LRAP to trim precursors to antigenic peptides in the endoplasmic reticulum (ER) following cleavage in the cytoplasm by tripeptidyl peptidase II [114]
MAGT1	3190625	3.7	Magnesium transporter 1	A critical regulator of basal intracellular free magnesium (Mg(2+)) concentrations [115]
MAL	4040398	3.7	T-cell differentiation protein	Highly hydrophobic integral membrane protein belonging to the MAL family of proteolipids. The protein has been localized to the endoplasmic reticulum of T-cells and is a candidate linker protein in T-cell signal transduction. In addition, this proteolipid is localized in compact myelin of cells in the nervous system and has been implicated in myelin biogenesis and/or function. The protein plays a role in the formation, stabilization and maintenance of glycosphingolipid-enriched membrane microdomains. Down-regulation of this gene has been associated with a variety of human epithelial malignancies [116]
MGC26356	3930255	2.7	Zinc finger protein 876, pseudogene	Not known
MRP63	750450	4	Mitochondrial ribosomal protein 63	Not known

($P < 0.05$) and *PAX8* ($P < 0.01$) (Figure 5A). However, *PROM1,* also known as the common ovarian cancer stem cell marker CD133, was not significantly enhanced in the CR group compared to the CN group in a set of 6 samples analysed although the trend of enhanced expression was evident. Although all three down regulated genes selected for validation, *SerpinA3*, *BCL11A* and *CRABP2*, did not show significant differences between the CN and CR groups, the decreasing trend in CR compared to CN group was evident (Figure 5B).

Changes in gene expression in As22D compared to As22C

Ascites 22C was obtained from a chemoresistant and recurring patient who had received sequential doses of chemotherapy listed in Table 1 (carboplatin and paclitaxel) (3 cycles), doxorubicin (4 cycles), AMG386 topotecan (2 cycles), cyclophosphamide (2 cycles). Ascites 22D was drained from the same patient within a month after the patient had received an additional cycle of cyclophosamide (number of chemotherapy cycles received = carboplatin and paclitaxel (3 cycles), doxorubicin (4 cycles), AMG386 topotecan (2 cycles), cyclophosphamide (3 cycles). Even though both samples overlapped each other in PCA plot (Figure 3B), some genetic differences was evident in the Heat Map (Figure 3A). On further investigation, 16 differentially expressed genes (8 up and down regulated in both cases) with a fold-change of >2-fold was observed in As22D compared to As22C. The genes are listed in Tables 5 and 6.

Ingenuity pathway analysis

To elucidate the underlying biological significance of DEGs identified by the microarray analysis between the CN and CR groups, Ingenuity Pathway Analysis was performed on the gene set identified using $FC > 2$ and $P < 0.05$ criteria. This was performed to identify the canonical pathways that uniquely regulate the chemoresistant phenotype of ascites tumor cells. With a data set of 414 DEGs (179 up regulated and 235 down regulated), 172 canonical pathways were identified. The gene content of the CR-associated 414 DEGs list corresponding to 433 probes was used for the generation of the biological networks using the Analyze Networks algorithm. The genes listed within the 414 DEG list were connected based upon their known relationship or

Table 6. 8 down regulated genes in As22C compared to As22D tumor cells (FC > 2)

Gene Symbol	Probe ID	FC	Gene Name	Gene Function
ADCY3	3800050	4.8	Adenylate cyclase 3	Membrane-associated protein which catalyzes the formation of cyclic adenosine-3′,5′-monophosphate (cAMP) [117]
ASS1	110433	3	Arginosuccinate synthetase	Rate limiting enzyme for arginine synthesis [118]
ASS1	2640544	3	Same as above	Same as above
C11orf63	1740767	7.5	chromosome 11 open reading frame 63	Uncharacterised protein
C3ORF34	1850040	4	centrosomal protein 19, also known as CEP19	This gene localizes to centrosomes and primary cilia and co-localizes with a marker for the mother centriole. This gene resides in a region of human chromosome 3 that is linked to morbid obesity [119]
IL-8	1570553	3.2	Interleukin-8	Pro-inflammatory tumor promoting cytokine [120]
IL-8	1980309	4.2	Same as above	Same as above
LCN2	4390398	3.5	Lipocalin -2, also known as neutrophil gelatinase-associated lipocalin (NGAL)	Adipokine/cytokine implicated in obesity and inflammation [121]
LRG1	6660162	2.3	Leucine-rich alpha-2-glycoprotein-1	Extracellular ligand for cytochrome C and acts as a survival factor [], In the presence of transforming growth factor-β1 (TGF-β1), is mitogenic to endothelial cells and promotes angiogenesis [122]
MT1A	6200402	2.8	Metallothionein 1A	Small, cysteine-rich proteins which have been implicated in various forms of stress providing cytoprotective action against oxidative injury, DNA damage and apoptosis [123]

functions associated with CR-dependent genes in the Ingenuity Pathways Knowledge Base. These networks were unique for CR-associated DEGs and are described in Supplementary Table 2. The majority of the pathways identified by Ingenuity Pathway Analysis were implicated in cancer, cellular growth and proliferation, cellular development, mitosis/cell cycle regulation, cellular assembly and organization. The top ten pathways are described in Table 7. Of these, the pathway regulated by the *PLK1* associated with Cell Cycle and DNA damage topped the list (Table 8). The principal genes involved in these pathways *CDC25c, CCNB1* and *PLK1* were all down regulated in CR tumors compared to CN tumors (Table 8). Potential involvement of *PLK*1, *CDC25c* and *CCNB1* in response to chemotherapy (DNA damage response) leading to G2-M cell cycle arrest and initiation of mitosis are depicted in Figures 6A and B.

DISCUSSION

To our knowledge, this is the first study which describes a genome wide microarray transcriptional profiling analysis on a small set of isolated tumor cells obtained from the ascites of advanced-stage CN and CR serous ovarian cancer patients. This was performed to specifically identify CR-associated genes and pathways that could be involved in the recurrence and subsequent progression of serous ovarian cancer. By combining our novel method of isolating ovarian tumor cells from the ascites of ovarian cancer patients with gene microarray analysis we were able to compare the gene expression profiles between CN and CR tumor cells without any back ground noise from the associated stromal cellular component.

Using the criterion FC > 2 and P < 0.05, this study demonstrated a unique gene expression profile of isolated tumor cells prior to and after chemotherapy as evidenced

Table 7. Top ten Ingenuity Pathway analysis

Ingenuity Canonical Pathways	P-value	Molecules involved
Mitotic Roles of Polo-Like Kinase	3.24E-05	*CDC25b, CDC25c, PLK-1, PPP2CB, CDC20, Cdk-1, CCNB1, ESPL1*
Cell-Cycle:G2/M DNA Damage Checkpoint Regulation	1.32E-04	*CDC25b, CDC25c, PLK-1, CDC20, CDK-1, CCNB1, CKS1B*
Role of Checkpoint Proteins in Cell Cycle Checkpoint Regulation	5.25E-04	*CDC25c, PLK-1, Cdk-1, PPP2CB, ATMIN,SLC19A1*
Lysine Degradation II	3.31E-03	*AASDHPPT, ALDH7A1*
Lysine Degradation V	3.31E-03	*AASDHPPT, ALDH7A1*
Herediatary Breast Cancer Signaling	5.89E-03	*CDC25c, Cdk-1, RB1, POLR2C, POLR2J, CCNB1, SLC19A1*
Acyl Carrier Protein Metabolism	1.86E-02	*AASDHPPT*
Asparagine Biosynthesis I	1.86E-02	*ASNS*
Protein Ubiquitination Pathway	2.09E-02	*USP14, USP3, Cdc20, DNAJC4, DNAJB14, DNAJB5, UBE2C, UBE2E3, UBE2L3*
Cholesterol Biosynthesis I	2.34E-02	*TM7SF2, SC5DL*

Table 8. Expression of common genes listed in the top three Ingenuity Pathway Analysis

Gene Symbol	Probe ID	P-value	FC (CR/CN)	Gene Name	Gene Function
CDC25C	3460152	0.0066	−4.71	cell division cycle 25C, also known as PPP1R60	This gene is highly conserved during evolution and it plays a key role in the regulation of cell division. It is a tyrosine phosphatase and directly dephosphorylates cyclin B-bound CDC2 and triggers entry into mitosis. It is also thought to suppress p53-induced growth arrest [112].
CDC25C	4200451	0.00126	−3.67	Same as above	Same as above
CDC25C	6110706	0.0254	−2.78	Same as above	Same as above
CCNB1	6450397	0.0448	−2.652	Cyclin B1	The gene product complexes with p34(cdc2) to form the maturation-promoting factor (MPF) that is expressed predominantly during G2/M phase [112]
CCNB1	4590040	0.0261	−2.566	Same as above	Same as above
PLK1	6130215	0.044	−2.680	Serine/threonine-Polo-like kinase 1	It is an early trigger for G2/M transition. It phosphorylates and activates CDC25C, a phosphatase that dephosphorylates and activates the cyclinB/CDC2 complex for entry of cells in G2-M phase [111, 112]

by the large number of DEGs (n = 414), of which 179 were up regulated and 235 were down regulated. The Heat Map and PCA analyses suggested a distinct separation with little overlap among the CR and CN associated genes. Overall, CR tumors displayed a unique up regulation of genes with functional relevance to cell-cell adhesion and tight junctions, embryonic development, cancer stem cells, tumor suppressor and genes involved in calcium and phospholipid signaling.

Claudins 1 (*CLDN1*) and 16 (*CLDN16*), which topped the up regulated list of genes, showed significant differences by validation at the mRNA level, are cell-cell

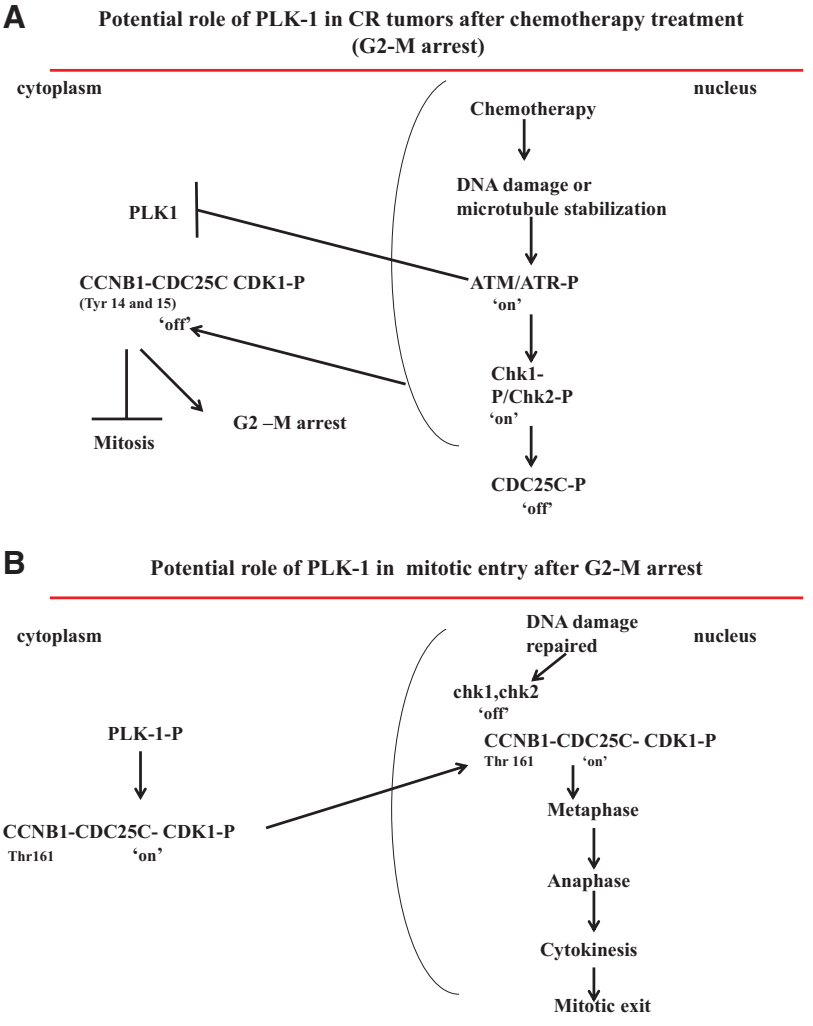

Figure 6. Potential involvement of *PLK1, CDC25c* and *CCNB1* in response to chemotherapy treatment in ascites-derived tumor cells. (A) In response to chemotherapy treatment ATM, ATR, chk1 and chk2 kinases are activated which causes nuclear exclusion of *CDC25c* in residual ascites-derived tumor cells. This results in mitotic arrest in preparation for DNA repair. PLK1 in that case is inactivated by active ATM or ATR response. **(B)** After DNA repair checkpoint kinases are silenced, phosphatases can reverse the inhibition enforced by checkpoint kinases so that *PLK1* can be activated with concomitant activation of *CCNB1-CDK1* complex. This results in the mitotic entry of cells with repaired DNA.

adhesion proteins that form the backbone of the apicolateral tight junctions and are crucial for epidermal barrier function [68]. These proteins are also essential for maintaining epithelial cell polarity [69]. In ovarian cancer, high expression of *CLDNS* 3, 4, 5 and 7 have been reported to be involved with tumorigenesis [70–72]. Over expression of *CLDN4* has also been shown to contribute to platinum resistance in ovarian cancer [73]. Even though significantly enhanced expression of *CLDN1* has been demonstrated in ovarian carcinoma effusions and is associated with poor survival [74], enhanced expression of *CLDN1* and *CLDN16* in CR compared to CN ascites-derived tumor cells has not been reported before.

Changes in gene expression profiles and corresponding epigenetic changes have been observed in cancer cells and embryonic stem cells [75, 76]. Hence, it was not surprising to note high expression of several embryonic stem cell genes in CR tumor cells, suggesting that therapy resistance programming of CR tumor cells may rely on the functional attributes of genes required for embryogenesis. Of the genes involved with embryogenesis, *ADAMTS9* was most up regulated (FC $>$ 22) [77]. *ADAMTS9* has been described as a tumor suppressor gene in a number of cancers including oesophageal and nasopharyngeal carcinoma [78]. In addition, *ADAMTS9* is also involved with the cleavage of proteoglycans such as versican and aggrecan [79]. Versican and aggrecan are important stromal components of ovarian carcinomas and have been shown to be involved with metastatic dissemination and angiogenesis of ovarian cancer cells [80]. Enhanced *ADAMTS9* expression in CR tumors may indicate low versican expression, due to higher proteolytic cleavage, resulting in the suppression of the stromal component and concomitant reduction in ovarian tumor cell dissemination outside the peritoneal environment [81]. This is consistent with our previous studies where we have demonstrated a relatively low stromal component in CR compared to CN ascites tumor cells [10]. Increased versican in the carcinoma stroma associates with poorer outcomes, possibly due to the facilitated migration of carcinoma cells away from the tumor [80, 81], and versican has also been shown to mediate mesenchymal epithelial transition to facilitate metastasis of breast carcinoma cells in the lungs [82–84].

We also demonstrate significantly higher expression of other embryonic and tumor suppressor genes such as *PAX8* [44], *TGFβR3* [85], and *UCA1* [42] in CR compared to CN tumor cells. Of these three genes, significantly enhanced expression of *PAX8* and *TGFβR3* was validated by qRT-PCR in CR ascites-derived tumor cells compared to CN tumor cells. *PAX8* is a lineage-restricted transcription factor that plays an essential role in the organogenesis of the Mullerian duct [86]. In the reproductive tract, *PAX8* expression is restricted to secretory cells of the fallopian tube epithelium [87], which recent reports have suggested as the cell of origin of serous ovarian cancer [88]. As such, *PAX8* has been shown to be overexpressed in ovarian cancers [87] and amplified in 16% of primary ovarian serous tumors [89]. Selective suppression of *PAX8* expression has been shown to induce apoptotic cell death in ovarian cancer cell lines, suggesting that *PAX8* is required for the proliferation of ovarian cancer cells [89]. Contrary to the expression of *PAX-8*, the expression of *TGFβR3* has been shown to be down-regulated in the majority of ovarian carcinomas and this was shown to be progressive with increasing tumor grade [90]. *TGFβR3* expression had been shown to have a significant inhibitory effect in ovarian cancer invasiveness, migration and the levels of MMP-2 and MMP-9 by promoting tumor suppressor effects of inhibin [90], as well as antagonizing the signals received by TGFβ [91, 92]. We have previously demonstrated that tumor cells from the ascites of CN and CR patients lack MMP-2 and MMP-9 expression [10]. This is also consistent with the immotile and non-aggressive nature of recurrent ovarian cancer where tumor growth is localized within the peritoneum microenvironment and is more dependent on dissemination by landing onto peritoneal organs rather than aggressive invasion through the vasculature [7]. As the expression of *TGFRβ3* is maintained by epigenetic transcriptional changes [90] it can be contemplated that CR tumor cells may undergo genetic reprogramming event under repetitive DNA damage repair processes resulting in cells with relatively high expression of *TGFRβ3* [93, 94]. However, the level of expression of the soluble form of *TGFβR3*, generated by ectodomain shedding of the cell surface receptor, yet remains to be investigated in the context of CN and CR tumors.

Ovarian cancer has been classified as a stem cell disease [95–97]. A recent study has presented a stem-like classification of high-grade serous tumors with poor patients' survival [98]. *PROM1* (CD133) a transmembrane glycoprotein has been defined as a marker for ovarian cancer stem cells [99], and the expression of *PROM1* in ovarian tumors has been associated with poor prognosis [100] and is directly regulated by epigenetic modification [101]. In our study, these observations were supported by the significantly enhanced expression of *PROM1* in CR (FC $>$ 9.30) compared to CN tumors by gene microarray. However, validation of *PROM1* in CR versus CN samples did not gain significance even though an increasing trend in CR samples was evident. This was probably due to the small number of samples tested for this study. We have also previously demonstrated enhanced expression of *PROM1* and other CSC markers in ovarian cancer cell lines and tumor cells isolated from the ascites of ovarian cancer patients in response to *in vitro* chemotherapy treatment [26, 27]. In addition, we have also demonstrated the emergence of CSC-like phenotype in mouse-xenograft models on intraperitoneal administration of chemotherapy after inoculation of ovarian cancer cells [27, 29, 97, 102]. These findings are consistent with the microarray data provided in Supplementary Table 1 which shows significant enhanced expression of *PDGFR*β and *JAG1*

among the top 30 genes in CR (FC > 4.80 and 4.30) compared to CN tumor cells. *PDGFR*β and *JAG1* have been associated with epithelial mesenchymal transition and CSCs in pancreatic cancer [103]. Thus, further studies on recurrent ovarian tumors in preclinical and clinical settings are needed to understand how CSC markers such as *PROM1*, *PDGFR*β and *JAG1* signals to support stem cell maintenance and tumor progression in the ascites microenvironment.

A unique down regulation of genes with functional relevance to protease inhibition, immunosuppressive tumor microenvironment, and energy and retinoic acid metabolism, regulator of cell cycle and mediator of anti-inflammatory reactions was observed in CR tumors. *SerpinA3* (FC > −26) topped the list among the down regulated proteins. *SerpinA3*, also known as alpha 1-antichymotrypsin is a member of the serpin super family, which inhibits the activity of certain proteases, such as cathepsin G in neutrophils and chymases in mast cells, by cleaving them into a different conformation [104]. Down regulation of *SerpinA3* expression may protect CR tumor cells from damage caused by neutrophil- and mast cell- associated proteolytic activities. Besides *SerpinA3*, other down regulated proteins such as *HCLS1* [105], *SOX18* [106], *LY96* [also known as myeloid differentiation factor -2 (MD-2)] [107], *HLA-DRB4* [53], and *BCL11A* [57] have been shown to be involved with lymphoangiogenesis, presentation of class II molecules to antigen presenting dendritic cells, and LPS signalling through Toll-like receptor 4. Down regulation of these molecules in CR tumor cells suggests that genes that regulate the activities of cytotoxic T cells, antigen presenting dendritic cells and differentiation of precursor endothelial cells associated with infiltrating lymphocytes are dominantly suppressed, suggesting that this mechanisms is used by CR tumors to escape host immune surveillance. These observations are consistent with the significant down regulation of *CD99*, a stromal factor expressed on cancer associated fibroblasts and stromal lymphocytes [108] again supporting reduced stromal/infiltrating T cell component in CR tumors as described before [10].

A particularly interesting observation in the CR gene list was the loss of *CRABP2* which previously has been shown to be over expressed in serous ovarian tumors [109]. Loss of *CRBP2* in CR tumors may indicate concomitant loss of vitamin A metabolism and retinoic acid receptor signalling required for differentiation of ascites tumor cells. Loss of *CRBP2* expression has been shown to be associated with decreased disease-free survival rates in Head and Neck Squamous Cell Carcinoma [110].

Interestingly, the two sequential chemotherapy samples obtained from the same CR patient (CR tumors-As22C and As22D) displayed close interaction in the PCA plot suggesting somewhat similar gene expression makeup. However, on further investigation 16 differentially genes were identified in these samples. Among these, genes like *APOF* [111], *KCNH6* [112], *KYNU* [113], *LRAP* [114], *MAGT1* [115], *MAL* [116], *MGC26356* and *MRP63* were up regulated by 2.7 to 5.3-folds in As22D compared to As22C. These up regulated proteins are involved with lipid transfer, voltage gated potassium channels, biosynthesis of NAD cofactor, magnesium transport and T-cell mediated immune functions. The down regulated genes included *ADCY3* [117], *ASS1* [118], *C11orf63*, *C3ORF34* [119], *IL-8* [120], LCN2 [121], *LRG1* [122] and *MT1A* [123] were down regulated by 2.3 to7.5-folds in As22D compared to As22C. Among the down regulated proteins IL-8 has been shown to have tumor promoting effect in ovarian cancer [120, 124]. It is not clear if the changes in the above genes is due to administration of a single dose of cyclophosmide to the patient or is it due to the *de novo* changes in the tumor during progression of the disease.

In order to identify 'dominant' pathways that may regulate the chemoresistant and chemonaive phenotype of ascites-derived tumor cells, we used Ingenuity Pathway Analysis. Of these, the mitotic pathways regulated by Polo-like kinase (*PLK1*), cell cycle: G2/M Damage checkpoint regulation and role of checkpoint proteins in cell cycle checkpoint control topped the list. *PLK*s are serine/threonine kinases, which are over expressed in many cancers and serve as biomarkers and a target for cancer therapy [125, 126]. *PLK*1 is expressed only in dividing cells from G2 onward and is degraded at the end of mitosis [125]. *PLK1* in combination with *CDC25c* and *CCNB1* regulates mitotic entry, spindle formation and cytokinesis in human cells [126]. *PLK1* also regulates G2-DNA damage checkpoint and is required for checkpoint recovery following checkpoint inactivation; that is when the damage is completely repaired and the cells restart the cell cycle [126]. *PLK1* has been shown as an independent prognostic marker for ovarian cancer patients [127] and *PLK2* as an epigenetic determinant of chemosensitivity and clinical outcomes in ovarian cancer [128].

In conclusion, we have demonstrated for the first time a unique and novel pattern of gene expression in isolated CR tumors compared to CN tumors obtained from the ascites of ovarian cancer patients. This preliminary study on a small sample size has utilised a systematic approach of studying only the tumor cells isolated from the ascites of CR and CN patients. We demonstrate an underlying lineage-specific relationship between high-grade serous ovarian carcinomas and ascites-derived tumor cells by the expression of lineage-specific essential gene *PAX8*. Unlike most other carcinomas, which dedifferentiate during progression and recurrence, recurrent ovarian tumors in the ascites microenvironment exist as epithelial cells in the form of spheroids [6, 10]. In that setting, up regulation of genes associated with cell-cell adhesion, embryonic stem cells, CSCs and genes antagonistic for migration and invasion (*TGFBR3*) defines the true characteristics of CR tumors in the ascites microenvironment. Concomitant down regulation of genes involved with host immune

surveillance provides an immunosuppressive environment that limits the host immune system to fight the tumor. This preliminary study, builds the framework of future studies, which will focus on particular genes and pathways of interest that may have therapeutic potential in reducing ascites-associated recurrences in ovarian cancer patients.

Conflict of interest: The authors declare that they have no competing interests.

AUTHOR'S CONTRIBUTION

AL designed the study, performed the experiments and contributed to the writing of the manuscript. RE designed the primers and contributed to the PCR experiments. MQ, EWT and JKF edited the manuscript; NA conceived the idea, designed the study and wrote the manuscript.

SUPPORTING INFORMATION

Table S1: Microarray expression data and gene ontology enrichment analyses.

Table S2: Ingenuity pathway networks of CR-associated DEGs.

ACKNOWLEDGEMENTS

The authors wish to thank Royal Women's Hospital Foundation, Women's Cancer Foundation, National Health and Medical Research Council of Australia (JKF, RegKey#441101), the Victorian Government's Operational Infrastructure Support Program (St. Vincent's Institute and MIMR-PHI Institute of Medical Research) and National Breast Cancer Foundation (EWT) for supporting this work. AL was the recipient of Royal Women's Hospital Scholarship. RE was supported by Marsha Rivkin Centre for Ovarian Cancer Research (NA).

REFERENCES

[1] Siegel R, Ward E, Brawley O, Jemal A. Cancer statistics, 2011: the impact of eliminating socioeconomic and racial disparities on premature cancer deaths. CA Cancer J Clin 2011, 61:212–236.

[2] Agarwal R, Kaye SB. Ovarian cancer: strategies for overcoming resistance to chemotherapy. Nat Rev Cancer 2003, 3:502–516.

[3] Gabra H. Back to the future: Targeting molecular changes for platinum resistance reversal. Gynecol Oncol 2010, 118:210–211.

[4] Kipps E, Tan DS, Kaye SB. Meeting the challenge of ascites in ovarian cancer: new avenues for therapy and research. Nat Rev Cancer 2013, 13:273–282.

[5] Ahmed N, Thompson EW, Quinn MA. Epithelial-mesenchymal interconversions in normal ovarian surface epithelium and ovarian carcinomas: an exception to the norm. J Cell Physiol 2007, 213:581–588.

[6] Shield K, Ackland ML, Ahmed N, Rice GE. Multicellular spheroids in ovarian cancer metastases: Biology and pathology. Gynecol Oncol 2009, 113:143–148.

[7] Lengyel E. Ovarian cancer development and metastasis. Am J Pathol 2010, 177:1053–1064.

[8] Hudson LG, Zeineldin R, Stack MS. Phenotypic plasticity of neoplastic ovarian epithelium: unique cadherin profiles in tumor progression. Clin Exp Metastasis 2008, 25:643–655.

[9] Ahmed N, Stenvers KL. Getting to Know Ovarian Cancer Ascites: Opportunities for Targeted Therapy-Based Translational Research. Front Oncol 2013, 3:256.

[10] Latifi A, Luwor RB, Bilandzic M, Nazaretian S, Stenvers K, Pyman J, Zhu H, Thompson EW, Quinn MA, Findlay JK, Ahmed N. Isolation and characterization of tumor cells from the ascites of ovarian cancer patients: molecular phenotype of chemoresistant ovarian tumors. PLoS One 2012, 7:e46858.

[11] Rizzo S, Hersey JM, Mellor P, Dai W, Santos-Silva A, Liber D, Luk L, Titley I, Carden CP, Box G, Hudson DL, Kaye SB, Brown R. Ovarian cancer stem like side populations are enriched following chemotherapy and overexpress EZH2. Mol Cancer Ther 2011, 10(2):325–335.

[12] Vathipadiekal V, Saxena D, Mok SC, Hauschka PV, Ozbun L, Birrer MJ. Identification of a potential ovarian cancer stem cell gene expression profile from advanced stage papillary serous ovarian cancer. PLoS One 2012, 7(1):e29079.

[13] Bamias A, Pignata S, Pujade-Lauraine E. Angiogenesis: a promising therapeutic target for ovarian cancer. Crit Rev Oncol Hematol 2012, 84:314–326.

[14] Liu JJ, Lu J, McKeage MJ. Membrane transporters as determinants of the pharmacology of platinum anticancer drugs. Curr Cancer Drug Targets 2012, 12:962–986.

[15] Shen DW, Pouliot LM, Hall MD, Gottesman MM. Cisplatin resistance: a cellular self-defense mechanism resulting from multiple epigenetic and genetic changes. Pharmacol Rev 2012, 64:706–721.

[16] Galluzzi L, Senovilla L, Vitale I, Michels J, Martins I, Kepp O, Castedo M, Kroemer G. Molecular mechanisms of cisplatin resistance. Oncogene 2012, 31:1869–1883.

[17] Jazaeri AA, Awtrey CS, Chandramouli GV, Chuang YE, Khan J, Sotiriou C, Aprelikova O, Yee CJ, Zorn KK, Birrer MJ, et al. Gene expression profiles associated with response to chemotherapy in epithelial ovarian cancers. Clin Cancer Res 2005, 11:6300–6310.

[18] Johnatty SE, Beesley J, Paul J, Fereday S, Spurdle AB, Webb PM, Byth K, Marsh S, McLeod H, Harnett PR, et al. ABCB1 (MDR 1) polymorphisms and progression-free survival among women with ovarian cancer following paclitaxel/carboplatin chemotherapy. Clin Cancer Res 2008, 14:5594–5601.

[19] Peters D, Freund J, Ochs RL. Genome-wide transcriptional analysis of carboplatin response in chemosensitive and chemoresistant ovarian cancer cells. Mol Cancer Ther 2005, 4:1605–1616.

[20] Balat O, Kudelka AP, Edwards CL, Verschraegen CF, Kavanagh JJ. Prolonged remission of platinum-refractory ovarian cancer with docetaxel: brief report and review of literature. Eur J Gynaecol Oncol 1997, 18:341–342.

[21] Berkenblit A, Seiden MV, Matulonis UA, Penson RT, Krasner CN, Roche M, Mezzetti L, Atkinson T, Cannistra SA. A phase II trial of weekly docetaxel in patients with platinum-resistant epithelial ovarian, primary peritoneal serous cancer, or fallopian tube cancer. Gynecol Oncol 2004, 95:624–631.

[22] Kavallaris M. Microtubules and resistance to tubulin-binding agents. Nat Rev Cancer 2010, 10:194–204.

[23] Mozzetti S, Ferlini C, Concolino P, Filippetti F, Raspaglio G, Prislei S, Gallo D, Martinelli E, Ranelletti FO, Ferrandina G, Scambia G. Class III beta-tubulin overexpression is a prominent mechanism of paclitaxel resistance in ovarian cancer patients. Clin Cancer Res 2005, 11:298–305.

[24] DeLoia JA, Zamboni WC, Jones JM, Strychor S, Kelley JL, Gallion HH. Expression and activity of taxane-metabolizing enzymes in ovarian tumors. Gynecol Oncol 2008, 108:355–360.

[25] Zaffaroni N, Pennati M, Colella G, Perego P, Supino R, Gatti L, Pilotti S, Zunino F, Daidone MG. Expression of the anti-

apoptotic gene survivin correlates with taxol resistance in human ovarian cancer. Cell Mol Life Sci 2002, 59:1406–1412.

[26] Ahmed N, Abubaker K, Findlay J, Quinn M. Cancerous ovarian stem cells: obscure targets for therapy but relevant to chemoresistance. J Cell Biochem 2013, 114(1):21–34.

[27] Abubaker K, Latifi A, Luwor R, Nazaretian S, Zhu H, Quinn MA, Thompson EW, Findlay JK, Ahmed N. Short-term single treatment of chemotherapy results in the enrichment of ovarian cancer stem cell-like cells leading to an increased tumor burden. Mol Cancer 2013, 12(1):24.

[28] Steg AD, Bevis KS, Katre AA, Ziebarth A, Dobbin ZC, Alvarez RD, Zhang K, Conner M, Landen CN. Stem cell pathways contribute to clinical chemoresistance in ovarian cancer. Clin Cancer Res 2012, 18(3):869–881.

[29] Abubaker K, Luwor R, Zhu H, McNally O, Quinn MA, Burns CJ, Thompson EW, Findlay JK, Ahmed N. Inhibition of the JAK2/STAT3 pathway in ovarian cancer results in the loss of cancer stem cell-like characteristics and a reduced tumor burden. BMC Cancer 2014, 14:217.

[30] Sherman-Baust CA, Becker KG, Wood Iii WH, Zhang Y, Morin PJ. Gene expression and pathway analysis of ovarian cancer cells selected for resistance to cisplatin, paclitaxel, or doxorubicin. J Ovarian Res 2011, 4:21.

[31] Armstrong SR, Narendrula R, Guo B, Parissenti AM, McCallum KL, Cull S, Lanner C. Distinct genetic alterations occur in ovarian tumor cells selected for combined resistance to carboplatin and docetaxel. J Ovarian Res 2012, 5:40.

[32] Ju W, Yoo BC, Kim IJ, Kim JW, Kim SC, Lee HP. Identification of genes with differential expression in chemoresistant epithelial ovarian cancer using high-density oligonucleotide microarrays. Oncol Res 2009, 18:47–56.

[33] Latifi A, Abubaker K, Castrechini N, Ward AC, Liongue C, Dobill F, Kumar J, Thompson EW, Quinn MA, Findlay JK, Ahmed N. Cisplatin treatment of primary and metastatic epithelial ovarian carcinomas generates residual cells with mesenchymal stem cell-like profile. J Cell Biochem 2011, 112:2850–2864.

[34] Kerr MK, Churchill GA. Experimental design for gene expression microarrays. Biostatistics 2001, 2:183–201.

[35] Yang YH, Speed T. Design issues for cDNA microarray experiments. Nat Rev Genet 2002, 3:579–588.

[36] Raychaudhuri S, Stuart JM, Altman RB. Principal components analysis to summarize microarray experiments: application to sporulation time series. Pac Symp Biocomput 2000:455–466.

[37] Bilandzic M, Chu S, Farnworth PG, Harrison C, Nicholls P, Wang Y, Escalona RM, Fuller PJ, Findlay JK, Stenvers KL. Loss of betaglycan contributes to the malignant properties of human granulosa tumor cells. Mol Endocrinol 2009, 23:539–548.

[38] Martin TA, Harrison GM, Watkins G, Jiang WG. Claudin-16 reduces the aggressive behavior of human breast cancer cells. J Cell Biochem 2008, 105:41–52.

[39] Stebbing J, Filipovic A, Giamas G. Claudin-1 as a promoter of EMT in hepatocellular carcinoma. Oncogene 2013.

[40] Kariya Y, Sato H, Katou N, Miyazaki K. Polymerized laminin-332 matrix supports rapid and tight adhesion of keratinocytes, suppressing cell migration. PLoS One 2012, 7:e35546.

[41] Lo PH, Lung HL, Cheung AK, Apte SS, Chan KW, Kwong FM, Ko JM, Cheng Y, Law S, Srivastava G, et al. Extracellular protease ADAMTS9 suppresses esophageal and nasopharyngeal carcinoma tumor formation by inhibiting angiogenesis. Cancer Res 2010, 70:5567–5576.

[42] Wang F, Li X, Xie X, Zhao L, Chen W. UCA1, a non-protein-coding RNA up-regulated in bladder carcinoma and embryo, influencing cell growth and promoting invasion. FEBS Lett 2008, 582:1919–1927.

[43] Hempel N, How T, Cooper SJ, Green TR, Dong M, Copland JA, Wood CG, Blobe GC. Expression of the type III TGF-beta receptor is negatively regulated by TGF-beta. Carcinogenesis 2008, 29:905–912.

[44] Tong GX, Devaraj K, Hamele-Bena D, Yu WM, Turk A, Chen X, Wright JD, Greenebaum E. Pax8. a marker for carcinoma of Mullerian origin in serous effusions. Diagn Cytopathol 2011, 39:567–574.

[45] Maitra R, Grigoryev DN, Bera TK, Pastan IH, Lee B. Cloning, molecular characterization, and expression analysis of Copine 8. Biochem Biophys Res Commun 2003, 303:842–847.

[46] Komuro A, Masuda Y, Kobayashi K, Babbitt R, Gunel M, Flavell RA, Marchesi VT. The AHNAKs are a class of giant propeller-like proteins that associate with calcium channel proteins of cardiomyocytes and other cells. Proc Natl Acad Sci U S A 2004, 101:4053–4058.

[47] Qiu G, Hill JS. Endothelial lipase enhances low density lipoprotein binding and cell association in THP-1 macrophages. Cardiovasc Res 2007, 76:528–538.

[48] Murakami Y, Kohyama N, Kobayashi Y, Ohbayashi M, Ohtani H, Sawada Y, Yamamoto T. Functional characterization of human monocarboxylate transporter 6 (SLC16A5). Drug Metab Dispos 2005, 33:1845–1851.

[49] Wagsater D, Johansson D, Fontaine V, Vorkapic E, Backlund A, Razuvaev A, Mayranpaa MI, Hjerpe C, Caidahl K, Hamsten A, et al. Serine protease inhibitor A3 in atherosclerosis and aneurysm disease. Int J Mol Med 2012, 30:288–294.

[50] Cavnar PJ, Mogen K, Berthier E, Beebe DJ, Huttenlocher A. The actin regulatory protein HS1 interacts with Arp2/3 and mediates efficient neutrophil chemotaxis. J Biol Chem 2012, 287:25466–25477.

[51] Duong T, Proulx ST, Luciani P, Leroux JC, Detmar M, Koopman P, Francois M. Genetic ablation of SOX18 function suppresses tumor lymphangiogenesis and metastasis of melanoma in mice. Cancer Res 2012, 72:3105–3114.

[52] Wu Y, Moser M, Bautch VL, Patterson C. HoxB5 is an upstream transcriptional switch for differentiation of the vascular endothelium from precursor cells. Mol Cell Biol 2003, 23:5680–5691.

[53] Marturano J, Longhi R, Casorati G, Protti MP. MAGE-A3(161-175) contains an HLA-DRbeta4 restricted natural epitope poorly formed through indirect presentation by dendritic cells. Cancer Immunol Immunother 2008, 57:207–215.

[54] Tsukamoto H, Fukudome K, Takao S, Tsuneyoshi N, Ihara H, Ikeda Y, Kimoto M. Multiple potential regulatory sites of TLR4 activation induced by LPS as revealed by novel inhibitory human TLR4 mAbs. Int Immunol 2012, 24:495–506.

[55] Veeranki S, Duan X, Panchanathan R, Liu H, Choubey D. IFI16 protein mediates the anti-inflammatory actions of the type-I interferons through suppression of activation of caspase-1 by inflammasomes. PLoS One 2011, 6:e27040.

[56] Schenkel AR, Mamdouh Z, Chen X, Liebman RM, Muller WA. CD99 plays a major role in the migration of monocytes through endothelial junctions. Nat Immunol 2002, 3:143–150.

[57] Yu Y, Wang J, Khaled W, Burke S, Li P, Chen X, Yang W, Jenkins NA, Copeland NG, Zhang S, Liu P. Bcl11a is essential for lymphoid development and negatively regulates p53. J Exp Med 2012, 209:2467–2483.

[58] Chen M, Zhang J, Li N, Qian Z, Zhu M, Li Q, Zheng J, Wang X, Shi G. Promoter hypermethylation mediated downregulation of FBP1 in human hepatocellular carcinoma and colon cancer. PLoS One 2011, 6:e25564.

[59] Cooper WN, Hesson LB, Matallanas D, Dallol A, von Kriegsheim A, Ward R, Kolch W, Latif F. RASSF2 associates

with and stabilizes the proapoptotic kinase MST2. Oncogene 2009, 28:2988–2998.

[60] Xing C, Xie H, Zhou L, Zhou W, Zhang W, Ding S, Wei B, Yu X, Su R, Zheng S. Cyclin-dependent kinase inhibitor 3 is overexpressed in hepatocellular carcinoma and promotes tumor cell proliferation. Biochem Biophys Res Commun 2012, 420:29–35.

[61] Hayakawa M, Matsushima M, Hagiwara H, Oshima T, Fujino T, Ando K, Kikugawa K, Tanaka H, Miyazawa K, Kitagawa M. Novel insights into FGD3, a putative GEF for Cdc42, that undergoes SCF(FWD1/beta-TrCP)-mediated proteasomal degradation analogous to that of its homologue FGD1 but regulates cell morphology and motility differently from FGD1. Genes Cells 2008, 13:329–342.

[62] Yan GR, Zou FY, Dang BL, Zhang Y, Yu G, Liu X, He QY. Genistein-induced mitotic arrest of gastric cancer cells by downregulating KIF20A, a proteomics study. Proteomics 2012, 12:2391–2399.

[63] Boimel PJ, Cruz C, Segall JE. A functional in vivo screen for regulators of tumor progression identifies HOXB2 as a regulator of tumor growth in breast cancer. Genomics 2011, 98:164–172.

[64] Baxter RM, Crowell TP, George JA, Getman ME, Gardner H. The plant pathogenesis related protein GLIPR-2 is highly expressed in fibrotic kidney and promotes epithelial to mesenchymal transition in vitro. Matrix Biol 2007, 26:20–29.

[65] Nguyen CH, Zhao P, Sobiesiak AJ, Chidiac P. RGS2 is a component of the cellular stress response. Biochem Biophys Res Commun 2012, 426:129–134.

[66] Jang CY, Coppinger JA, Yates JR 3rd, Fang G. Phosphoregulation of DDA3 function in mitosis. Biochem Biophys Res Commun 2010, 393:259–263.

[67] Rao RG, Sudhakar D, Hogue CP, Amici S, Gordon LK, Braun J, Notterpek L, Goodglick L, Wadehra M. Peripheral myelin protein-22 (PMP22) modulates alpha 6 integrin expression in the human endometrium. Reprod Biol Endocrinol 2011, 9:56.

[68] Furuse M, Hata M, Furuse K, Yoshida Y, Haratake A, Sugitani Y, Noda T, Kubo A, Tsukita S. Claudin-based tight junctions are crucial for the mammalian epidermal barrier: a lesson from claudin-1-deficient mice. J Cell Biol 2002, 156:1099–1111.

[69] Morin PJ. Claudin proteins in human cancer: promising new targets for diagnosis and therapy. Cancer Res 2005, 65:9603–9606.

[70] Kwon MJ, Kim SS, Choi YL, Jung HS, Balch C, Kim SH, Song YS, Marquez VE, Nephew KP, Shin YK. Derepression of CLDN3 and CLDN4 during ovarian tumorigenesis is associated with loss of repressive histone modifications. Carcinogenesis 2010, 31:974–983.

[71] Turunen M, Talvensaari-Mattila A, Soini Y, Santala M. Claudin-5 overexpression correlates with aggressive behavior in serous ovarian adenocarcinoma. Anticancer Res 2009, 29:5185–5189.

[72] Kim CJ, Lee JW, Choi JJ, Choi HY, Park YA, Jeon HK, Sung CO, Song SY, Lee YY, Choi CH, et al. High claudin-7 expression is associated with a poor response to platinum-based chemotherapy in epithelial ovarian carcinoma. Eur J Cancer 2011, 47:918–925.

[73] Yoshida H, Sumi T, Zhi X, Yasui T, Honda K, Ishiko O. Claudin-4: a potential therapeutic target in chemotherapy-resistant ovarian cancer. Anticancer Res 2011, 31:1271–1277.

[74] Kleinberg L, Holth A, Trope CG, Reich R, Davidson B. Claudin upregulation in ovarian carcinoma effusions is associated with poor survival. Hum Pathol 2008, 39:747–757.

[75] Ben-Porath I, Thomson MW, Carey VJ, Ge R, Bell GW, Regev A, Weinberg RA. An embryonic stem cell-like gene expression signature in poorly differentiated aggressive human tumors. Nat Genet 2008, 40:499–507.

[76] Calvanese V, Horrillo A, Hmadcha A, Suarez-Alvarez B, Fernandez AF, Lara E, Casado S, Menendez P, Bueno C, Garcia-Castro J, et al. Cancer genes hypermethylated in human embryonic stem cells. PLoS One 2008, 3:e3294.

[77] Jungers KA, Le Goff C, Somerville RP, Apte SS. Adamts9 is widely expressed during mouse embryo development. Gene Expr Patterns 2005, 5:609–617.

[78] Enomoto H, Nelson CM, Somerville RP, Mielke K, Dixon LJ, Powell K, Apte SS. Cooperation of two ADAMTS metalloproteases in closure of the mouse palate identifies a requirement for versican proteolysis in regulating palatal mesenchyme proliferation. Development 2010, 137:4029–4038.

[79] Boeuf S, Graf F, Fischer J, Moradi B, Little CB, Richter W. Regulation of aggrecanases from the ADAMTS family and aggrecan neoepitope formation during in vitro chondrogenesis of human mesenchymal stem cells. Eur Cell Mater 2012, 23:320–332.

[80] Ween MP, Oehler MK, Ricciardelli C. Role of Versican, Hyaluronan and CD44 in Ovarian Cancer Metastasis. Int J Mol Sci 2011, 12:1009–1029.

[81] Ghosh S, Albitar L, LeBaron R, Welch WR, Samimi G, Birrer MJ, Berkowitz RS, Mok SC. Up-regulation of stromal versican expression in advanced stage serous ovarian cancer. Gynecol Oncol 2010, 119:114–120.

[82] Ween MP, Hummitzsch K, Rodgers RJ, Oehler MK, Ricciardelli C. Versican induces a pro-metastatic ovarian cancer cell behavior which can be inhibited by small hyaluronan oligosaccharides. Clin Exp Metastasis 2011, 28:113–125.

[83] Sheng W, Wang G, La Pierre DP, Wen J, Deng Z, Wong CK, Lee DY, Yang BB. Versican mediates mesenchymal-epithelial transition. Mol Biol Cell 2006, 17:2009–2020.

[84] Gao D, Vahdat LT, Wong S, Chang JC, Mittal V. Microenvironmental regulation of epithelial-mesenchymal transitions in cancer. Cancer Res 2012, 72:4883–4889.

[85] Finger EC, Turley RS, Dong M, How T, Fields TA, Blobe GC. TbetaRIII suppresses non-small cell lung cancer invasiveness and tumorigenicity. Carcinogenesis 2008, 29:528–535.

[86] Mittag J, Winterhager E, Bauer K, Grummer R. Congenital hypothyroid female pax8-deficient mice are infertile despite thyroid hormone replacement therapy. Endocrinology 2007, 148:719–725.

[87] Bowen NJ, Logani S, Dickerson EB, Kapa LB, Akhtar M, Benigno BB, McDonald JF. Emerging roles for PAX8 in ovarian cancer and endosalpingeal development. Gynecol Oncol 2007, 104:331–337.

[88] Karst AM, Levanon K, Drapkin R. Modeling high-grade serous ovarian carcinogenesis from the fallopian tube. Proc Natl Acad Sci U S A 2011, 108:7547–7552.

[89] Cheung HW, Cowley GS, Weir BA, Boehm JS, Rusin S, Scott JA, East A, Ali LD, Lizotte PH, Wong TC, et al. Systematic investigation of genetic vulnerabilities across cancer cell lines reveals lineage-specific dependencies in ovarian cancer. Proc Natl Acad Sci U S A 2011, 108:12372–12377.

[90] Hempel N, How T, Dong M, Murphy SK, Fields TA, Blobe GC. Loss of betaglycan expression in ovarian cancer: role in motility and invasion. Cancer Res 2007, 67:5231–5238.

[91] Bandyopadhyay A, Wang L, Lopez-Casillas F, Mendoza V, Yeh IT, Sun L. Systemic administration of a soluble betaglycan suppresses tumor growth, angiogenesis, and matrix metalloproteinase-9 expression in a human xenograft model of prostate cancer. Prostate 2005, 63:81–90.

[92] Dong M, How T, Kirkbride KC, Gordon KJ, Lee JD, Hempel N, Kelly P, Moeller BJ, Marks JR, Blobe GC. The type III TGF-

beta receptor suppresses breast cancer progression. J Clin Invest 2007, 117:206–217.

[93] Mossman D, Kim KT, Scott RJ. Demethylation by 5-aza-2′-deoxycytidine in colorectal cancer cells targets genomic DNA whilst promoter CpG island methylation persists. BMC Cancer 2010, 10:366.

[94] Lengauer C, Kinzler KW, Vogelstein B. DNA methylation and genetic instability in colorectal cancer cells. Proc Natl Acad Sci U S A 1997, 94:2545–2550.

[95] Curley MD, Garrett LA, Schorge JO, Foster R, Rueda BR. Evidence for cancer stem cells contributing to the pathogenesis of ovarian cancer. Front Biosci 2011, 16:368–392.

[96] Aguilar-Gallardo C, Rutledge EC, Martinez-Arroyo AM, Hidalgo JJ, Domingo S, Simon C. Overcoming Challenges of Ovarian Cancer Stem Cells: Novel Therapeutic Approaches. Stem Cell Rev 2012, 8(3):994–1010.

[97] Ahmed N, Abubaker K, Findlay JK. (2013) Ovarian cancer stem cells: Molecular concepts and relevance as therapeutic targets. Mol Aspects Med 2013 Jun 25. doi:pii: S0098-2997(13)00042-3. 10.1016/j.mam.2013.06.002. [Epub ahead of print].

[98] Schwede M, Spentzos D, Bentink B, Hofmann O, Haibe-Kains B, Harrington D, Quackenbush J, Culhane AC. Stem cell-like gene expression in ovarian cancer predicts type II subtype and prognosis. PLOS ONE 2013, 8:e57799.

[99] Silva IA, Bai S, McLean K, Yang K, Griffith K, Thomas D, Ginestier C, Johnston C, Kueck A, Reynolds RK, et al. Aldehyde dehydrogenase in combination with CD133 defines angiogenic ovarian cancer stem cells that portend poor patient survival. Cancer Res 2011, 71:3991–4001.

[100] Zhang J, Guo X, Chang DY, Rosen DG, Mercado-Uribe I, Liu J. CD133 expression associated with poor prognosis in ovarian cancer. Mod Pathol 2012, 25:456–464.

[101] Baba T, Convery PA, Matsumura N, Whitaker RS, Kondoh E, Perry T, Huang Z, Bentley RC, Mori S, Fujii S, et al. Epigenetic regulation of CD133 and tumorigenicity of CD133+ ovarian cancer cells. Oncogene 2009, 28:209–218.

[102] Abubaker K, Luwor RB, Escalona R, McNally O, Quinn MA, Thompson EW, Findlay JK, Ahmed N. Targeted disruption of JAK2/STAT3 pathway in combination with systemic administration of paclitaxel inhibits the priming of ovarian cancer stem cells leading to a reduced tumor burden. Front Oncol 2012, 4:75.

[103] Wang Z, Li Y, Kong D, Banerjee S, Ahmad A, Azmi AS, Ali S, Abbruzzese JL, Gallick GE, Sarkar FH. Acquisition of epithelial-mesenchymal transition phenotype of gemcitabine-resistant pancreatic cancer cells is linked with activation of the notch signaling pathway. Cancer Res 2009, 69:2400–2407.

[104] Kalsheker NA. Alpha 1-antichymotrypsin. Int J Biochem Cell Biol 1996, 28:961–964.

[105] Scielzo C, Ten Hacken E, Bertilaccio MT, Muzio M, Calissano C, Ghia P, Caligaris-Cappio F. How the microenvironment shapes chronic lymphocytic leukemia: the cytoskeleton connection. Leuk Lymphoma 2010, 51:1371–1374.

[106] Eom BW, Jo MJ, Kook MC, Ryu KW, Choi IJ, Nam BH, Kim YW, Lee JH. The lymphangiogenic factor SOX 18: a key indicator to stage gastric tumor progression. Int J Cancer 2012, 131:41–48.

[107] Gray P, Dagvadorj J, Michelsen KS, Brikos C, Rentsendorj A, Town T, Crother TR, Arditi M. Myeloid differentiation factor-2 interacts with Lyn kinase and is tyrosine phosphorylated following lipopolysaccharide-induced activation of the TLR4 signaling pathway. J Immunol 2011, 187:4331–4337.

[108] Edlund K, Lindskog C, Saito A, Berglund A, Ponten F, Goransson-Kultima H, Isaksson A, Jirstrom K, Planck M, Johansson L, et al. CD99 is a novel prognostic stromal marker in non-small cell lung cancer. Int J Cancer 2012, 131:2264–2273.

[109] Toyama A, Suzuki A, Shimada T, Aoki C, Aoki Y, Umino Y, Nakamura Y, Aoki D, Sato TA. Proteomic characterization of ovarian cancers identifying annexin-A4, phosphoserine aminotransferase, cellular retinoic acid-binding protein 2, and serpin B5 as histology-specific biomarkers. Cancer Sci 2012, 103:747–755.

[110] Calmon MF, Rodrigues RV, Kaneto CM, Moura RP, Silva SD, Mota LD, Pinheiro DG, Torres C, de Carvalho AF, Cury PM, et al. Epigenetic silencing of CRABP2 and MX1 in head and neck tumors. Neoplasia 2009, 11:1329–1339.

[111] Lagor WR, Fields DW, Khetarpal SA, Kumaravel A, Lin W, Weintraub N, Wu K, Hamm-Alvarez SF, Drazul-Schrader D, de la Llera-Moya M, Rothblat GH. the effects of apolipoprotein F defiency on high density lipoprotein cholesterol metabolism in mice. PLoS One 2012, 7:e31616.

[112] Pardo LA, Contreras-Jurado C, Zientkowska M, Alves F, Stuhmer W. Role of voltage-gated potassium channels in cancer. J Membr Biol 2005, 205:115–124.

[113] Goode G, Pratap S, Eltom SE. Depletion of aryl hydrocarbon receptor in MDA-MB-231 human breast cancer cells altered the expression of genes in key regulatory pathways of cancer. PLoS One 2014, 9:e3100103.

[114] Li H, Takai N, Yuge A, Furukaewa Y, Tsuno A, Tsukamoto Y, Kong S, Moriyama M, Narahara H. Novel target genes responsive to the anti-growth activity of triptolide in endometrial and ovarian cancer cells. Cancer Lett 2010, 297:198–206.

[115] Chaigne-Delalande B, Li FY, O'Çonnor GM, Lukacs MJ, Joiang P, Zheng L, Shatzer A, Biancalana M, Pittaluga S, Matthews HF, et al. Mg2+ regulates cytotoxic functions of NK and CD8 T cells in chronic EBV infection through NKG2D. Science 2013, 341:186–191.

[116] Eguchi D, Ohuchida K, Kozono S, Ikenaga N, Shindo K, Cui L, Fujiwara K, Akagawa S, Ohtsuka T, Takahata S, et al. MAL2 expression predicts distant metastasis and short survival in pancreatic cancer. Surgery 2013, 154:573–582.

[117] Hong SH, Goh SH, Lee SJ, Hwang JA, Lee J, Choi IJ, Seo H, Park JH, Suzuki H, Yamamoto E, et al. Upregulation of adenylate cyclase 3 (ADCY3) increases the tumorigenic potential of cells by actoivating the CREB p[athway. Oncotarget 2013, 4:1791–1803.

[118] McAlpine JA, Lu HT, Wu KC, Knowles SK, Thomson JA. Down-regulation of arginosuccinate is associated with cisplatin resistance in heptocellular carcinoma cell lines: implications for PEGylated arginine deiminase combination therapy. BMC Cancer 2014, 14:621.

[119] Shalata A, Ramirez MC, Desnick RJ, Priedigkeit N, Buettner C, Lindner C, Mahroum M, Abdul-Ghani M, Dong F, Arar N, et al. Morbid obesity resulting from inactivation of the ciliary protein CEP19 in humans and mice. Am J Hum Genet 2013, 93:1061–1071.

[120] Lane D, Matte I, Rancout C, Piche A. Prognostic significance of Il-6 and Il-8 ascites levels in ovarian cancer patients. BMC Cancer 2011, 11:210.

[121] Lippi G, Meschi T, Nouvenne A, Mattiuzzi C, Borghi L. Neutrophil gelatinase-associated lipocalin in cancer. Adv Clin Chem 2014, 64:179–219.

[122] Wang X, Abraham S, McKenzie JA, Jeffs N, Swire M, Tripathi VB, Luhmann UF, Lange CA, Zhai Z, Arthur HM, et al. LRG1 promotes angiogenesis by modulating endothelial TGF-β signalling. Nature 2013, 4899:306–311.

[123] Jakovac H, Tota M, Grebic D, Grubic-Kezele T, Barac-Latas V, Mrakovcic-Sutic, Milin C, Radosevic-Stasic B. Metallothionein I+II expression as an early sign of chronic relapsing

experimental autoimmune encephalomyelitis in rats. Curr Aging SCi 2013:37–44.

[124] Yigit R, Figdor CG, Zusterzeel PL, Pots JM, Torensma R, Massuger LF. Cytokine analysis as a tool to understand tumour-host interaction in ovarian cancer. Eur J Cancer 2011, 47:1883–1889.

[125] Weiss L, Efferth T. Polo-like kinase 1 as target for cancer therapy. Exp Hematol Oncol 2012, 1:38.

[126] van Vugt MA, Medema RH. Getting in and out of mitosis with Polo-like kinase-1. Oncogene 2005, 24:2844–2859.

[127] Weichert W, Denkert C, Schmidt M, Gekeler V, Wolf G, Kobel M, Dietel M, Hauptmann S. Polo-like kinase isoform expression is a prognostic factor in ovarian carcinoma. Br J Cancer 2004, 90:815–821.

[128] Syed N, Coley HM, Sehouli J, Koensgen D, Mustea A, Szlosarek P, McNeish I, Blagden SP, Schmid P, Lovell DP, et al. Polo-like kinase Plk2 is an epigenetic determinant of chemosensitivity and clinical outcomes in ovarian cancer. Cancer Res 2011, 71:3317–3327.